

MICROCOPY

100-10

12

AFGL-TR-85-0336

MATHEMATICAL AND STATISTICAL ANALYSIS

F. Battles
P. Burkhardt
A. Campbell

E. Good
M. B. Hulit
D. Kerr

P. Moss
E. Murphy
K. Scharr

AD-A169 277

Bedford Research Associates
4 DeAngelo Drive
Bedford, MA 01730

October 1985

Final Report
September 1982 - October 1985

DTIC
SELECTED
JUL 03 1986
S D
V D

APPROVED FOR PUBLIC RELEASE; DISTRIBUTION UNLIMITED

AIR FORCE GEOPHYSICS LABORATORY
AIR FORCE SYSTEMS COMMAND
UNITED STATES AIR FORCE
HANSCOM AIR FORCE BASE, MASSACHUSETTS 01731

DTIC FILE COPY

28

1

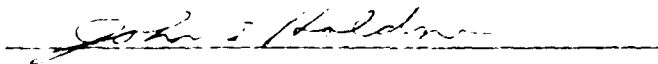
This report has been reviewed by the ESD Public Affairs Office (PA) and is releasable to the National Technical Information Service (NTIS).

This technical report has been reviewed and is approved for publication.



PAUL TSIPOURAS
Contract Manager

FOR THE COMMANDER



LT COL J.E. Holdner, Director
Research Services Division

Qualified requestors may obtain additional copies from the Defense Technical Information Center. All others should apply to the National Technical Information Service.

If your address has changed, or if you wish to be removed from the mailing list, or if the addressee is no longer employed by your organization, please notify AFGL/DAA, Hanscom AFB, MA 01731. This will assist us in maintaining a current mailing list.

Do not return copies of this report unless contractual obligations or notices on a specific document requires that it be returned.

Unclassified

SECURITY CLASSIFICATION OF THIS PAGE (When Data Entered)

REPORT DOCUMENTATION PAGE		READ INSTRUCTIONS BEFORE COMPLETING FORM	
1. REPORT NUMBER AFGL-TR-85-0336	2. GOVT ACCESSION NO. A-D-H169277	3. RECIPIENT'S CATALOG NUMBER	
4. TITLE (and Subtitle) Mathematical and Statistical Analysis		5. TYPE OF REPORT & PERIOD COVERED FINAL REPORT Sept. 1982 - Oct. 1985	
		6. PERFORMING ORG. REPORT NUMBER FINAL REPORT	
7. AUTHOR(s) F. Battles E. Good P. Moss P. Burkhardt M.B. Hulit E. Murphy A. Campbell D. Kerr K. Scharr		8. CONTRACT OR GRANT NUMBER(s) F19628-82-0139	
9. PERFORMING ORGANIZATION NAME AND ADDRESS BEDFORD RESEARCH Associates 4 DeAngelo Drive Bedford, MA 01730		10. PROGRAM ELEMENT, PROJECT, TASK AREA & WORK UNIT NUMBERS 62101F 9993XXAI	
11. CONTROLLING OFFICE NAME AND ADDRESS Air Force Geophysics Laboratories Hanscom AFB, Massachusetts 01731 Monitor: Paul Tsipouras, AFGL/SIA		12. REPORT DATE October 1985	
		13. NUMBER OF PAGES 112	
14. MONITORING AGENCY NAME & ADDRESS (if different from Controlling Office)		15. SECURITY CLASS. (of this report) Unclassified	
		15a. DECLASSIFICATION DOWNGRADING SCHEDULE	
16. DISTRIBUTION STATEMENT (of this Report) Approved for public release; distribution unlimited.			
17. DISTRIBUTION STATEMENT (of the abstract entered in Block 20, if different from Report)			
18. SUPPLEMENTARY NOTES			
19. KEY WORDS (Continue on reverse side if necessary and identify by block number) One-minute instantaneous rainfall, Infrared emission, Turbopause height, Gravity analysis, Borehole well, Cn ² , Rawinsonde data, Defense Meteorological Satellite Program.			
20. ABSTRACT (Continue on reverse side if necessary and identify by block number) This report presents a summary of analyses and mathematical modeling done in support of some AFGL atmospheric research projects. In particular, work on modeling 1-min instantaneous rainfall fates, infrared emissions, turbopause height analysis, gravity analysis, gaussian smoothing of Cn ² , rawinsonde data processing, borehole well log analysis and the defense meteorological satellite program processing are discussed.			

DD FORM 1473
1 JAN 73

Unclassified

SECURITY CLASSIFICATION OF THIS PAGE (When Data Entered)

TABLE OF CONTENTS

	Page
Defense Meteorological Satellite Program Processing	5
C_n^2 Calculations from Rawinsonde Data Using the VanZandt and Kaimal Models	18
Rawinsonde Data Processing	24
Gaussian Smoothing of C_n^2 Observations from Day and Night Flights	33
Turbopause Height Study	53
Instantaneous Rainfall Analysis	57
Gravity Analysis	83
Theory and Modeling of Infrared Emission	100
Borehold Log Plotting and Analysis	105

Accession For	
NTIS CRA&I	<input checked="" type="checkbox"/>
DTIC TAB	<input type="checkbox"/>
Unannounced	<input type="checkbox"/>
Justification	
By _____	
Distribution/	
Availability Codes	
Dist	Avail and/or Special
A-1	

DEFENSE METEOROLOGICAL SATELLITE PROGRAM PROCESSING

1.0 INTRODUCTION

1.1 Background

BEDFORD RESEARCH Associates' work on the "J4", "J*", "IE", and "M" experiments of the Defense Meteorological Satellite Program (DMSP) which consists of processing raw data tapes, and creating/maintaining applications programs. The data from the F2 through F7 satellites is put onto DM tapes at Offut Air Force Base, Nebraska. These tapes are shipped to the Air Force Geophysics Laboratory (AFGL) for processing by BEDFORD RESEARCH Associates and the Space Physics Division. Each experiment's data is first processed by a program designed to create a database (this is Phase 1). Phase 2 consists of creating interactive programs to use this data. BEDFORD RESEARCH Associates designs these programs and maintains the "J4" and "J*" databases.

2.0 PROJECT DESCRIPTION

Each experiment has a database interactive package and an applications interactive package. Each experiment's database package has the following essential options: 1) an option to merge ten DM tapes onto one tape, and 2) an option to take up to five of the latter and reduce the data to a standard format. The latter process is called a production run. Other options are also present in the database packages, depending on the experiment. The applications programs for each experiment are similar. The following describes the interactive packages in more detail.

2.1 "J4" Database Interactive Package

The procedure which runs the "J4" database interactive package is J4INTCR. When this command is issued, the user will be prompted with a series of questions that enable him to create one of the following batch jobs:

- 1) Merge ten DM tapes to one tape
- 2) Create a database by using up to five of option 1's tapes
- 3) Create a Computer Center (CC) tape of data from up to five of option 2's tapes

Backups of the CC tapes are also made by BEDFORD RESEARCH Associates personnel and kept at the base office.

The tapes from option 1 are given a magnetic label of HAX followed by three numbers. The paper label is BR followed by three numbers. All tapes, except the CC tapes, are supplied by BEDFORD RESEARCH Associates. These tapes are reduced to standard format by half-months for each satellite (F6 and F7) by using option 2.

Option 2, a production run, prompts the user for the satellite desired. It also prompts the user for the beginning or end of a month. The range for the beginning of the month is day 1 through day 15; the range for the end of the month is day 16 through day 31. The tape is given a magnetic label of BR as well as a paper label of BR. An example of a multifile label on a production run tape is B1APR85F6 (beginning of April [1-15], 1985, satellite F6).

These production run tapes are then copied to a CC tape by option 3. These CC tapes contain up to five half-months of data. For example, the end of February, 1985 through the end of April, 1985 for satellite F7 might be on one CC tape. The data for F6 and F7 production runs are kept separate. These CC tapes are used by the Space Physics Division for the applications interactive package. They are also backed up by BEDFORD RESEARCH personnel in case a CC tape is destroyed. For a brief outline of the components of the J4 database interactive package, see Appendix A.

2.2 "J*" Database Interactive Package

The "J*" database interactive package is similar to the one for "J4". Ten DM tapes are merged onto one tape with a magnetic label of STR followed by three numbers. The paper label is a BR label.

These tapes are then reduced to standard format and put onto an OS tape. The OS number is supplied by the computer center. Unlike "J4", a whole month of data is put on an OS tape. Also, only the F7 satellite is involved.

These OS tapes are further reduced by packing the data. The data on one OS tape is packed and put onto another OS tape. These OS tapes are used by the Space Physics Division in the applications programs. These tapes are also backed up by BEDFORD RESEARCH Associates. For an outline of the "J*" database package, see Appendix B.

2.3 "IE" Database Interactive Package

The "IE" database interactive package, used by the Space Physics Division, has five options. The first option merges the data and the second reduces it onto DMM tapes by half-months. Option 3, however, used the production runs to create four files of reduced data: Ion Sweep, Electron Sweep, Ion Density, and Electron Density. Option 4 allows one to copy the information from Option 2 or 3 onto a tape for use in the applications package. Option 5 copies a tape for backup purposes. See Appendix C for an outline of the components of the "IE" database package.

2.4 "M" Database Interactive Package

The "M" database package has three options. The first merges ten raw data tapes onto one tape. The second reduces these to one DMM tape. This tape is then copied to a CC tape and backed up. This package is very similar to the "J4" package. However, two versions of the "M" package are used by the Space Physics Division — one for data prior to January 13, 1985, and one for data for Jan. 13 - Jan. 31. The data format changed to ASCII and subsequently the packages were changed. See Appendix D for an outline of the two versions.

2.5 "J4" Applications Interactive Package

There are four options in this package: list, flux, spec, and file. List creates a listing of the requested data. Flux creates flux plots of ion and electron data. Spec creates spectra plots, and file creates a file of distribution, differential flux, or counts data. All options can be run for whole day intervals or specific time periods of less than a day. Also, if one chooses the flux option, one can obtain a printout of the values of JTOT, JETOT, and EAVE.

These options use the CC tapes created by the database packages. The procedure file creates a batch job, which is a local file. This file can then be routed by the user. See Appendix E for an outline of the package.

2.6 "J*" Applications Interactive Package

There are seven options in the "J*" package. Each can be run for intervals in whole days or for smaller time periods. The options include the following: 1) list, 2) print sums of counts, doses or fluxes, 3) file, 4) survey plots, 5) output non-zero star counts, 6) polar pass averages, and 7) polar plots. See Appendix F for an outline of the package's components.

2.7 "IE" Applications Interactive Package

This is very similar to the "J4" package. It has three options: list, flux, and file. There is no spectra option. See Appendix G for an outline of the components of the package.

2.8 "M" Applications Interactive Package

This is also very similar to the J4 package. However, there are five options: list, flux, spec, file, and magf. The latter generates plots of the magnetic files. See Appendix H for an outline of the components of the package.

2.9 Summary of Packages

Basically, there are four data base packages and four applications packages. BEDFORD RESEARCH Associates maintains two of the data bases. The applications programs are used by the Space Physics Division of AFGL. They also maintain the "M" and "IE" databases. All the packages are for the F6 and F7 satellites, except for the "J*" package which is for the F7 only.

3.0 PROCESSING ACCOMPLISHED

Data processing has been done on the following:

- IE - from November 1983
- J* - from November 1983
- J4 - from December 1982
- M - from November 1983

4.0 ADDITIONAL EFFORTS

It had also been requested that a file option for "J4" be created to contain the ephemeris and data for the electrons, channels 1-13, for satellite F7. Also, the values JETOT, JTOT, EAVE, Σ_p and Σ_H have been calculated, printed, and put in a file. The following are the formulas for the last three values:

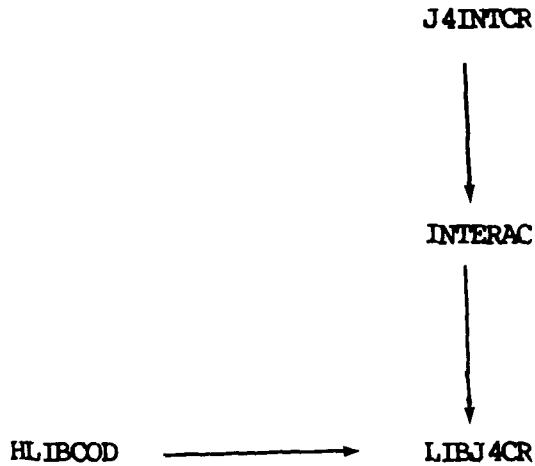
$$EAVE = \frac{JETOT}{JTOT} = E_0$$

$$\Sigma_p = I \frac{1/2 \quad 2\theta E_0}{E \quad (4+E_0^2)}, \text{ where } I_E = 2 \pi 1.602 \times 10^{-10} JETOT$$

$$\Sigma_H = E_0 \quad \Sigma_p \quad 5/8$$

APPENDIX A

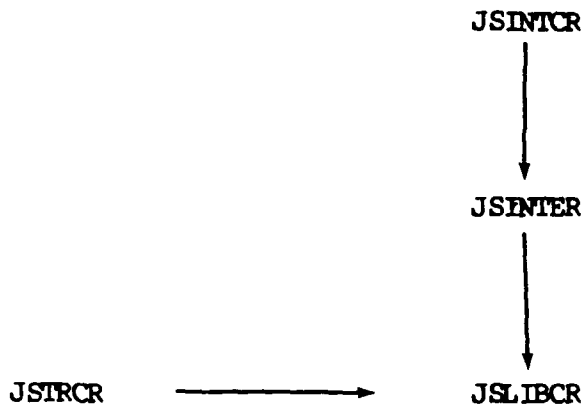
"J4" DATABASE INTERACTIVE PACKAGE



- J4INTCR: Procedure file which runs the package
- INTERAC: FORTRAN program which creates the batch file
- LIBJ4CR: Library of FORTRAN code which merges, reduces, and copies the data.
- HLIBCOD: FORTRAN code which merges, reduces, and copies the data.

APPENDIX B

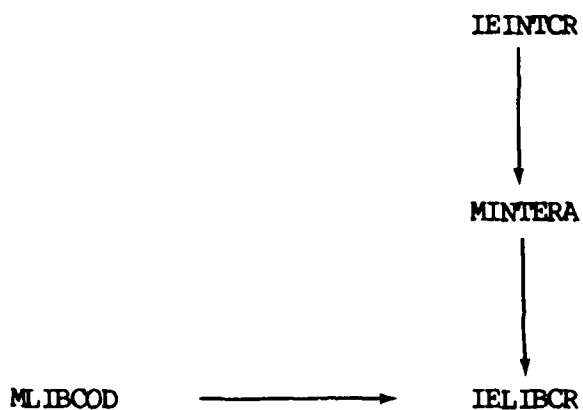
"J*" DATABASE INTERACTIVE PACKAGE



- JSINTCR: Procedure which runs the package
- JSINTER: FORTRAN code which creates the batch job
- JSLIBCR: Library code of JSIRCR
- JSIRCR: FORTRAN code which merges, reduces, packs and copies the data

APPENDIX C

"IE" DATABASE INTERACTIVE PROGRAM



- IEINTCR: Procedure to run the package
- MINTERA: FORTRAN code which creates a batch job
- IELIBCR: Library of code of MLIBCOD
- MLIBCOD: FORTRAN code which merges, reduces, and copies the data

APPENDIX D

"M" DATABASE INTERACTIVE PACKAGES



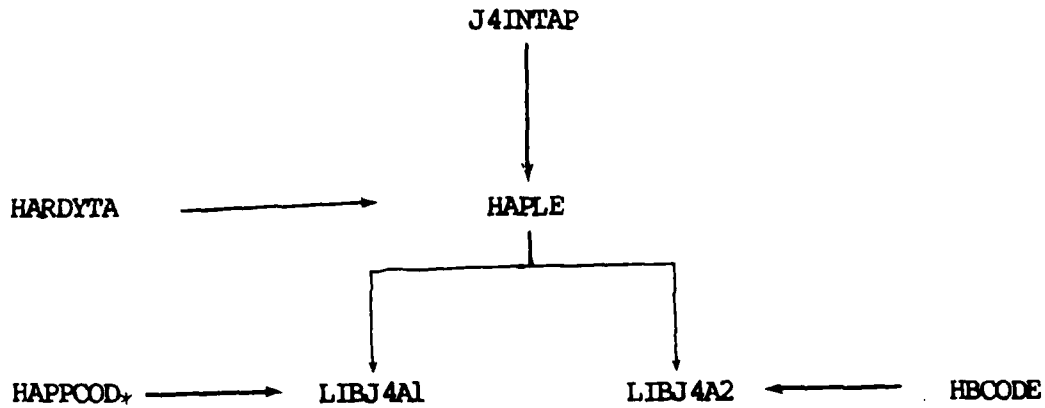
* uses magfldd

** uses IGRF80

- MDICOLD, MDINTER: Procedures which run the packages
- OLDMIC, MDINTER: FORTRAN programs which create batch jobs
- MDLIBCX, MDLIBCI: Libraries of FORTRAN code
- MDLIBCO, MDLIBCR: FORTRAN codes which merge, reduce, and copy data

APPENDIX E

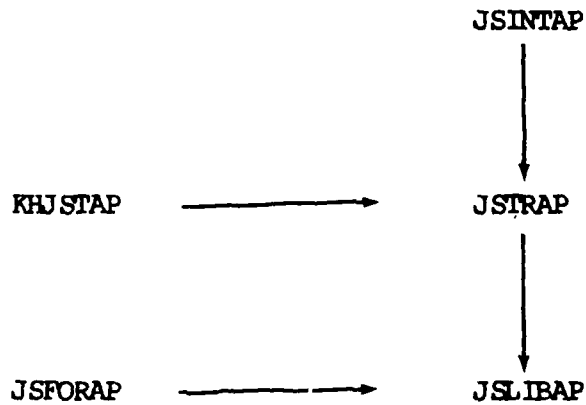
"J4" APPLICATIONS INTERACTIVE PACKAGE



- J4INTAP: Procedure which runs the package
- HAPLE: FORTRAN code which creates the batch job
- HARDYTA: List of data tapes available for use
- LIBJ4A1: Library of code for list, flux, and spec options
- LIBJ4A2: Library of code for file option
- HAPPCOD: List, flux, and spec FORTRAN code
- HBCODE: File FORTRAN code

APPENDIX F

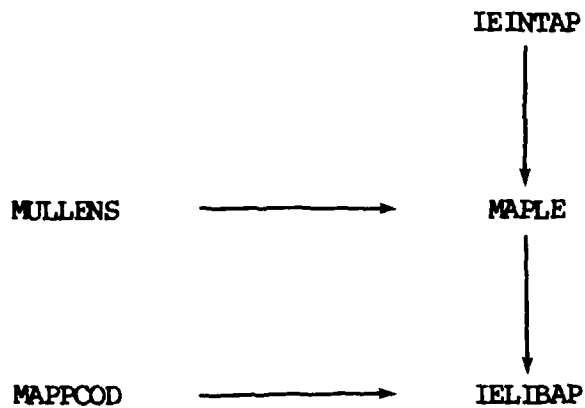
"J*" APPLICATIONS INTERACTIVE PACKAGE



- JSINTAP: Procedure to run the package
- JSTRAP: FORTRAN code to create batch job
- KHJSTAP: List of tapes available
- JSLIBAP: Library of code
- JSFORAP: Code to produce the data for plotting, etc.

APPENDIX G

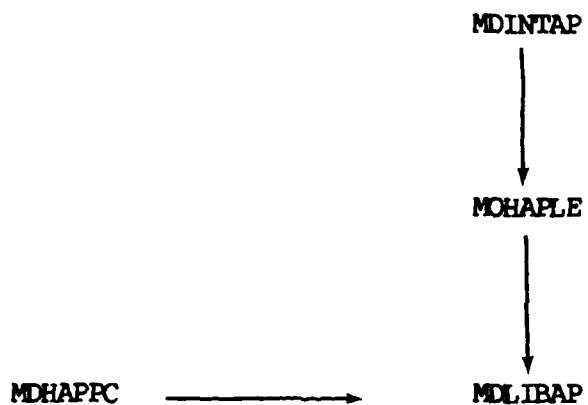
"IE" APPLICATIONS INTERACTIVE PACKAGE



IEINTAP: Procedure which runs package
MAPLE: FORTRAN code which creates batch job
MULLENS: List of tapes available
IELIBAP: Library of code
MAPPCOD: Code which processes data for an option

APPENDIX H

"M" APPLICATIONS INTERACTIVE PROGRAM



- MDINTAP: Procedure which runs package
- MDHAPLE: FORTRAN code which creates the batch job
- MDLIBAP: Library of code
- MDHAPPC: Code to process data for options

Cn² CALCULATIONS FROM RAWINSONDE DATA USING THE VANZANDT AND KAIMAL MODELS

1.0 INTRODUCTION

1.1 Overview

C_n^2 , the refractivity structure constant, is the most important parameter in determining the effects of clear-air turbulence on optical beam propagation. Various optical properties, such as the transverse coherence length and the isoplanatic angle, are determined from altitude weighted integrals of C_n^2 through the atmosphere down to the observation point.^{1,2,4} The dominant contribution to these integrals will usually be from the atmospheric boundary layer but the contribution from the free atmosphere, especially in the presence of a strong jet stream is not negligible. Also, the existence of a strong temperature inversion layer, marking the transition from the boundary layer to the free atmosphere, can contribute significantly to the integrals.

1.2 Background

Various methods exist for obtaining altitude profiles for C_n^2 , such as thermosonde radar and stellar scintillometers. To develop seasonal profiles at various locations throughout North America which could be used in best/worst case studies, for example, it is desirable to develop methods of calculating C_n^2 from rawinsonde measurements of temperature, pressure and wind velocities. The main advantage is the extremely low cost per rawinsonde launch as compared to other more direct but expensive techniques used to determine C_n^2 . Models developed using the larger rawinsonde data base can be compared to measurements from these other techniques to determine reliability. In the application of rawinsonde data to obtain C_n^2 estimates, we have made use of two models, one for the free atmosphere and the other for the boundary layer to calculate C_n^2 from 0.1 km up to 4 km.

2.0 DATA

For the model development, we have used measurements from standard

rawinsondes that were modified to telemeter temperature data at a higher rate than is normally obtained and required for weather reporting purposes. The higher resolution is required here in order to determine accurately the first temperature inversion layer above the ground for purposes explained further in discussions of the models used. These data were obtained by personnel at the Pacific Missile Test Center, California.

The measurements were made at 3 sites within 75 miles of one another in the proximity of Los Angeles, California. A total of 81 balloon launches were made in September of 1983, 43 from Pt. Mugu, 14 from El Segundo and 24 from San Nicholas Island. The rawinsonde measurements were made at roughly 0.1 km increments. The pressure, temperature and wind velocities were then smoothed using a cubic spline fit.⁵ The fitted data was then used to evaluate C_n^2 from the models discussed in the next section.

3.0 ANALYSIS

The model used for the free atmosphere was that developed by VanZandt and coworkers.⁷ An extensive discussion of this model and how it can be used in conjunction with rawinsonde data is provided in reference 6. The upper limit used was arbitrarily chosen as 4 km but could easily be extended up to where the balloon bursts, which is typically 25 to 30 kilometers. It is assumed that the lower limit on this model is at the bottom of the first strong temperature inversion layer. This should mark the transition from the boundary layer to the free atmosphere.

The model used for the boundary layer contribution is due to Kaimal and coworkers.³ As modified by Walters and Kunkel,⁸ the model takes the form:

$$\frac{C_n^2(z)}{C_n^2(z_0)} = \begin{cases} (z/z_0)^{-4/3} & z_0, z \leq 0.5z_i \\ (.5z_i/z_0)^{-4/3} & 0.5z_i \leq z < 0.7z_i \\ 2.9(.5z_i/z_0)^{-4/3}(z/z_i)^3 & 0.7z_i \leq z_i \end{cases}$$

The model is expected to work best when there is a well-defined temperature inversion present, which was true for about 2/3 of the launches. There are two parameters built into this model: Z_i , the height of the inversion layer, and $C_n^2(z_0)$, the value of C_n^2 at some height z_0 .

A computer algorithm is used to determine Z_i from the imputed smoothed temperature values (at 0.1 km increments) by searching for the first occurrence (if any) of a negative temperature gradient. This height is taken as the height of the inversion base if:

- a) the temperature gradient remains negative for the next two 0.1 km increments and drops by at least 1° ,
- or
- b) the temperature drops by more than 2° .

When a temperature inversion is found, Z_i has been of order 0.5 km, with some occurrences of Z_i up to order 2.5 km. No inversion is found in about 1/3 of the launches.

A series of temperature plots were done for three launches at Pt. Mugu on September 28, 1983. These are representative of a well-defined, relatively high-altitude, inversion layer. This layer appears to move upward and lose definition as the day progresses. Another plot illustrates a launch for which there is apparently no inversion, while a third plot illustrates a weakly defined inversion layer at about 0.7 km, which does not meet the selecting criteria of the above algorithm. This is probably all right, since this inversion is so weakly defined that the Kaimal model may not be applicable.

The second parameter, $C_n^2(z_0)$ (i.e., an accurate measure of C_n^2 down in the stable region of the boundary layer), was not available. In the absence of such a measurement, the VanZandt model was used to calculate C_n^2 at the bottom of the inversion layer. We then require that the Kaimal model give the same value at this point. With this modification we have:

$$\frac{C_n^2(z)}{C_n^2(z_i)} = \begin{cases} .136 (z/z_i)^{-4/3} & z \leq .5z_i \\ .343 & .5z_i \leq z \leq .7z_i \\ (z/z_i)^3 & .7z_i \leq z \leq z_i \end{cases}$$

where $C_n^2(z_i)$ is obtained from the VanZandt model. Should accurate values of C_n^2 at an appropriate height become available, we could easily go back to the original formulation.

4.0 RESULTS

For 25 of the 80 launches, a well-defined temperature inversion was located above 1 km. For each of these we calculated C_n^2 from 4 km down to the inversion layer using the VanZandt model. We then forced the Kaimal model to match the VanZandt model at this point and then used it to calculate C_n^2 down to 0.1 km.

The upper limit of 4 km is quite arbitrary in that, typically, the data needed for the VanZandt model is available up to at least 20 km. The lower limit of 0.1 km is somewhat arbitrary in that it is not clear how far down the Kaimal model can be used. The use of relatively high (above 1 km) inversion layers was made to show the contrast between the boundary layer and the free atmosphere.

For contrast, we have also the Kaimal model to calculate C_n^2 from the inversion layer down to 0.1 km. However, it must be remembered that this model is not valid in this regime.

A typical result for C_n^2 along with the associated temperature profile shows a well-defined inversion beginning at 2.5 km. Graphically, below the inversion layer, the improper extension of the VanZandt model is noted for comparison to the better suited Kaimal model.

Analysis of three nearly simultaneous launches from three launch sites show that for each set, although the structure of the temperature profile through the inversion differ, the height is approximately the same. A peak in C_n^2 is also common for each of the three launches.

It might be more desirable to use the original formulation of the Kaimal model instead of the one used, even though the two are mathematically equivalent. Forcing the Kaimal model to join the VanZandt model will affect all the other values obtained below z_i . For a launch analyzed,

changing Z_i to 2.9 km or 3.1 km will affect the C_n^2 values below Z_i by several orders of magnitude. Were an accurate value of C_n^2 available for $Z < 0.5Z_i$, this problem could be avoided.

5.0 SUMMARY

The high resolution rawinsonde data obtained at the three stations in the Los Angeles area provided extremely good examples of well established temperature inversion layers which generally were present in the early afternoon. This fits well with conditions described by Kaimal³ and the application of the modified Kaimal model by Walters and Kunkel⁸.

We have calculated C_n^2 as a function of altitude when a well-defined temperature inversion layer is present at altitudes of 1-3 km. We used the VanZandt model down to the inversion layer and the Kaimal model below. One of the parameters in the Kaimal model is determined from the VanZandt model; the other parameter (the inversion layer height) is obtained from the smoothed temperature profile. Should independent measurements of the first of these parameters become available, our procedure can easily be modified to take advantage of it.

REFERENCES

1. Fante, R.L., 1975: Electromagnetic Beam Propagation in Turbulent Media, Proc. IEEE, 63, 1669-1692.
2. Hufnagel, R.E., 1978: Propagation Through Atmospheric Turbulence in The Infrared Handbook, U.S. Government Printing Office, Washington, DC, Chap. 6, 6-1-6-56.
3. Kaimal, J.C. et al, 1976: Turbulence Structure in the Convective Boundary Layer, J. of Atm. Sci., 33, 2152-2169.
4. Lawrence, R.S. and Strohbehn, J.W., 1970: A Survey of Clear-Air Propagation Relevant to Optical Communications, Proc. IEEE, 58, 1523-1545.
5. Murphy, E.A., D'Agostino, R.E. and Noonan, J.P., 1982: Patterns in the Occurrence of Richardson Numbers Less Than Unity in the Lower Atmosphere, J. Appl. Meteor., 21, 321-333.
6. Murphy, E.A. et al, 1984: C_n^2 (Optical) Studies in the Free Atmosphere Based on Rawinsonde Data, AFGL-TR-84-0135 ADA147307
7. VanZandt, T.E., Gage, K.S. and Warnock, J.M., 1981: An Improved Model for the Calculation of Profiles of C_n^2 and ϵ in the Free Atmosphere from Background Profiles of Wind, Temperature and Humidity, Reprints 20th Conf., Radar Meteor. Soc., Boston, Amer. Meteor. Soc., 129-135.
8. Walters, D.L. and Kunkel, K.E., 1981: Atmospheric Transfer Function for Desert and Mountain Locations: The Atmospheric Effects on τ_o , J. Opt. Soc. Am., 71, 397-405.

RAWINSONDE DATA PROCESSING

1.0 INTRODUCTION

During the past year, BEDFORD RESEARCH personnel transferred rawinsonde balloon data, called "Clear1" and "Clear2", from floppy disks to the CDC Cyber System. These files were edited and then dumped to an ANSI standard labeled tape which was later brought to White Sands, New Mexico. The following is an in-depth report on the details of this project.

2.0 DATA PROCESSING

2.1 Overview

The original eighty-eight data files were converted to ASCII code and put on five and one-quarter inch floppy disks. These files were transferred to the Cyber System (see Appendix A for a list of the files). They were kept as direct-access files because the total prus for indirect-access files for that account was insufficient. The following describes the original data in detail.

2.2 Data Descriptiton

Each Clear1 and Clear2 data file consists of three parts. The first two are header records; the third consists of the actual data records. These parts are described below in more depth.

The first header record consists of five fields. These fields contain the date, time, serial number, latitude, and longitude. The following is an example of the first header records (see Appendix B for the format):

09-078421:11:34m1882 +32.40000+106.3700

The second header record is divided into two records for writing purposes. The first contains these surface parameters: altitude, pressure, temperature, humidity, wind speed, wind direction, C_n^2 , and 10^{σ}ex^2 . The second contains R_{φ} , O_{φ} , vrms, zfinal, gmt offset, and the number of data records (see Appendix C for formats). The following is an example of the second header record:

```
1216.2 875.1+31.6 + 22. 6.2+300.+4.43E-14+0.00E+00
+2.8 +3.4 +16.724.75 +6 999
```

The third part consists of the actual data records. In the original Clear data, the fields were altitude, pressure, temperature, humidity, C_n^2 , the logarithm of the average C_n^2 , σ of the logarithm of the average C_n^2 , the east displacement, the north displacement, wind speed, and wind direction (see Appendix D for the formats of the original files). The following is an example of a data record in the Clear1 and Clear2 files:

```
11.000 238.3-40.0 +21+2.27E-18+1.74E-18+1.27E+00 -9.99 -9.99 +23.1+271
```

2.3 Data Manipulation

The original files were edited by a FORTRAN program. The new files have the same fields, excluding the logarithm of the average C_n^2 , σ of the logarithm of the average C_n^2 , the east displacement, and the north displacement (see Appendix E for a list of the new files and Appendix F for the formats of the new files). The following is an example of a data record in the Clear1 and Clear2 files:

```
11.000 250.2-40.0 +21+2.27E-18 +23.1+271
```

A few items concerning the new files should be noted. If there was no data gathered for the humidity, C_n^2 , or the wind direction, the field received the value -999. If the wind speed had no data for that altitude, the value -999.9 was given to the data. Also, the file Om5315b contains two different data sets, which run together due to no end-of-file marker. The original data was in this format for this file.

2.4 Data Tape Creation

The original and new files were dumped to CC tapes. Another tape, which was taken to White Sands, New Mexico, has the new files on it. The tape sent to White Sands was an ANSI standard labeled tape. It was a nine-track tape with a density of 6250 bits per inch. There was a volume header label, a header label, and an end-of-file label on the tape. No end-of-volume label was necessary.

Each file was copied to the tape in coded form until the end-of-file marker was reached. Each end-of-file marker determines the end of one file and the beginning of another. However, each file is considered one record. The maximum block size was set to 10,000.

3.0 SUMMARY

The transferral of the Clear1 and Clear2 files to the Cyber system took place in May, 1985. The editing and creation of the tape, along with the documentation, was completed in June.

The tape which was sent to White Sands may be recreated. It may be easier to use the present CC tapes, or to create a CC tape again.

APPENDIX A

List of Files

M0503	M1888	M2770	M6415
M0506	M1889	M2771	M6416
M0507	M1890	M6371	M6417
M0508	M1891	M6372	M6420
M0516	M1892	M6373	M6425
M0517	M1893	M6381	M6548
M0518	M1895	M6383	M6550
M0522	M1896	M6384	M6555
M0524	M2694	M6385	M6557
M0527	M2703	M6386	M6558
M0534	M2710	M6387	M6561
M0543	M2711	M6388	M6562
M0546	M2712	M6389	M6563
M0547	M2754	M6392	M6564
M1692	M2757	M6395	OM5308
M1878	M2758	M6398	OM5315b
M1879	M2759	M6403	OM5316
M1880	M2762	M6406	OM5317
M1882	M2763	M6408	OM5319
M1884	M2764	M6409	OM5321
M1885	M2766	M6410	OM5322
M1886	M2769	M6412	OM5323

APPENDIX B

First Header Record

field	columns	format	
date	1-8	I2.2,'-',I2,'-',I2	+++
time	10-16	I2.2,':',I2.2,':',I2.2	+++
* serial number	17-21	A5	+
latitude	26-33	F8.4	++
longitude	34-42	F9.4	++

* OM files have six-character serial numbers, and OM5315A has a seven-character serial number.

- + Character format with specified length
- ++ Single precision floating point real without exponent
- +++ Integer with specified length

APPENDIX C

Second Header Record

Part_1

field	columns	format
surface altitude	1-6	F6.1 **
surface pressure	7-12	F6.1 **
surface temperature	13-17	F5.1 **
surface humidity	18-22	F5.0 **
surface windspeed	23-26	F4.1 **
surface wind direction	27-31	F5.0 **
Cn2	28-36	E9.2 *
10 ⁿ ex2	37-45	E9.2 *

Part_2

R _φ	1-6	F6.1 **
O _φ	7-12	F6.1 **
VRMS	13-18	F6.1 **
zfinal	19-23	F5.2 **
gmt offset	24-26	I3 ***
# of data records	27-30	I4 ***

- * Single precision floating point real with exponent
- ** Single precision floating point real without exponent
- *** Integer with specified length

APPENDIX D

Original Data Format

field	columns	format
altitude	1-6	F6.3 **
pressure	7-12	F6.1 **
temperature	13-17	F5.1 **
humidity	18-21	I4 ***
C_n^2	22-30	E9.2 *
logarithm of average C_n^2	31-39	E9.2 *
σ of logarithm of average C_n^2	40-48	E9.2 *
east displacement	49-55	F7.2 **
north displacement	56-62	F7.2 **
wind speed	63-68	F6.1 **
wind direction	69-72	I4 ***

* Single precision floating point real with exponent

** Single precision floating point real without exponent

*** Integer with specified length

APPENDIX E

List of Files

M0503B	M1888B	M2770B	M6 41 5B
M0506B	M1889B	M2771B	M6 41 6B
M0507B	M1890B	M6371B	M6 41 7B
M0508B	M1891B	M6372B	M6 420B
M0516B	M1892B	M6373B	M6 425B
M0517B	M1893B	M6381B	M6548B
M0518B	M1895B	M6383B	M6550B
M0522B	M1896B	M6384B	M6555B
M0524B	M2694B	M6385B	M6557B
M0527B	M2703B	M6386B	M6558B
M0534B	M2710B	M6387B	M6561B
M0543B	M2711B	M6388B	M6562B
M0546B	M2712B	M6389B	M6563B
M0547B	M2754B	M6392B	M6564B
M1692B	M2757B	M6395B	OM5308B
M1878B	M2758B	M6398B	OM5315B
M1879B	M2759B	M6403B	OM5316B
M1880B	M2762B	M6406B	OM5317B
M1882B	M2763B	M6408B	OM5319B
M1884B	M2764B	M6409B	OM5321B
M1885B	M2766B	M6410B	OM5322B
M1886B	M2769B	M6412B	OM5323B

APPENDIX F

New Data Format

field	columns	format
altitude	1-6	F6.3 **
pressure	7-12	F6.1 **
temperature	13-17	F5.1 **
humidity	18-21	I4 ***
C_n^2	22-30	E9.2 *
wind speed	31-36	F6.1 ***
wind direction	37-40	I4 ***

- * Single precision floating point real with exponent
- ** Single precision floating point real without exponent
- *** Integer with specified length

GAUSSIAN SMOOTHING OF C_n^2 OBSERVATIONS FROM DAY AND NIGHT FLIGHTS

1.0 INTRODUCTION

1.1 Overview

This report outlines the ADP support that Bedford Research Associates provided the Atmospheric Optics Branch (OPA) of the Air Force Geophysics Laboratory (AFGL). It describes the nature of the analyses as well as the software used in this investigation.

1.2 Background and Objectives

One measure of atmospheric turbulence is the optical refractory constant, C_n^2 . This index is subject to a variety of meteorological events such as, temperature, wind, pressure, and relative humidity. Each of these events have been used in the prediction of C_n^2 variation. One condition that has received little empirical study is the differential effects of day and night sampling on C_n^2 measures. It is the purpose of this investigation to examine and report the daily and nightly patterns of C_n^2 data.

The tasks developed to analyze these data are presented below:

- * Download data files from tape to disk
- * Edit downloaded files to exclude cases with missing data and adjust noise C_n^2 values.
- * Write the algorithms to calculate:
 - Running means of C_n^2 for individual flights
 - Grand (pooled) C_n^2 means from the individual flights
 - Gaussian smoothed C_n^2 scores from individual and pooled data sets
 - Regression coefficients for the pooled mean values using log quadratic and nonlinear equations
- * Plot individual and pooled C_n^2 values by altitude
- * Write an output file containing altitude and gaussian smoothed scores to tape

1.3 Report Outline

This report is divided into three sections. The first section provides a description of the software designed to perform the tasks listed in Section 1.2. In this part of the report, the software requirements, functions

executed by the main program, and structure of the original and edited data files are reviewed. The next section identifies and describes the results of the analyses performed. The third, and final section, summarizes the findings of this study.

2.0 SOFTWARE SYSTEM

2.1 Overview

This section outlines the functional characteristics of the software developed to compute the running means and gaussian smoothed C_n^2 values from individual and aggregated day or night flights. It describes the software requirements used to create this system. It also delineates the operations (i.e., inputs, processing, and outputs) within the main program and presents the format of the data files.

2.2 Requirements

In the initial stages of software development, a number of programming requirements were specified. These requirements were used in constructing the algorithms and source code for the main program. Each of these constraints are discussed below:

- * Records containing missing altitude and/or C_n^2 data were omitted from any computations. These cases provided inaccurate information that could distort the calculations of mean or smoothed C_n^2 scores.
- * C_n^2 observations with noise were adjusted using the following equation:

$$C_n^2 = (79.9 * P / (T^2) * 10^{-6})^2 * C_T^2$$

where P = pressure (mb)
T = temperature (K)
 $C_T^2 = (.002)^2$

This formula resulted in values of C_n^2 that could be used in subsequent computations. If the pressure and/or temperature were missing, the case was excluded from further processing.

- * Mean and gaussian values were estimated on cases that contained an altitude window (or standard deviation) of 20 or 40 meters (m).

Thus, to be included in these calculations, an altitude level of 10 or 20 m above the lowest, and below the highest, points was required. Cases that did not fall within this region were omitted because they did not contain a full window.

- * The gaussian smoothing of individual day and night flights were done on the raw C_n^2 scores contained within each file. However, the grand smoothing of n flights was performed on the average C_n^2 values.
- * Results were plotted on the Calcomp Plotter or written to a tape file containing the pooled smoothed C_n^2 scores plus their corresponding altitude levels for day and night flights.

2.3 Software Functions

All software was developed and executed on the AFGL Control Data Corporation (CDC) 170/750 Cyber mainframe running under NOS 2.3. The source code for the main program was written in ANSI standard Fortran (Version 5.0). Routines were also coded using NOS command language for file management and IMSL libraries were used to obtain the regression coefficients.

The software operations were implemented on the individual and pooled data files. Therefore, the following discussion will address each of these activities independently. A flowchart is presented in Figure 2.3.1 to describe the ADP activity.

2.3.1 Individual Flight Operations

2.3.1.1 Inputs

The inputs to the individual flight computations were obtained from the downloaded tape files. These files were in binary format and are described in more detail in Section 2.4. The inputs to the algorithm were the flight number, altitude, temperature, pressure, and raw C_n^2 observations.

2.3.1.2 Processing

The data was first sorted by altitude in ascending order and then read into an algorithm that calculated mean and smoothed C_n^2 scores. At the beginning of this process, the integrity of each observation was checked. Records with missing or outlying values were deleted from the file and those with noise C_n^2 recording were corrected. The records that passed through this editing stage were entered into an array of valid cases. An altitude window was constructed for each element in the array. If data points contained a full window of 20 or 40 m, they were used to compute the mean and smoothed C_n^2 values.

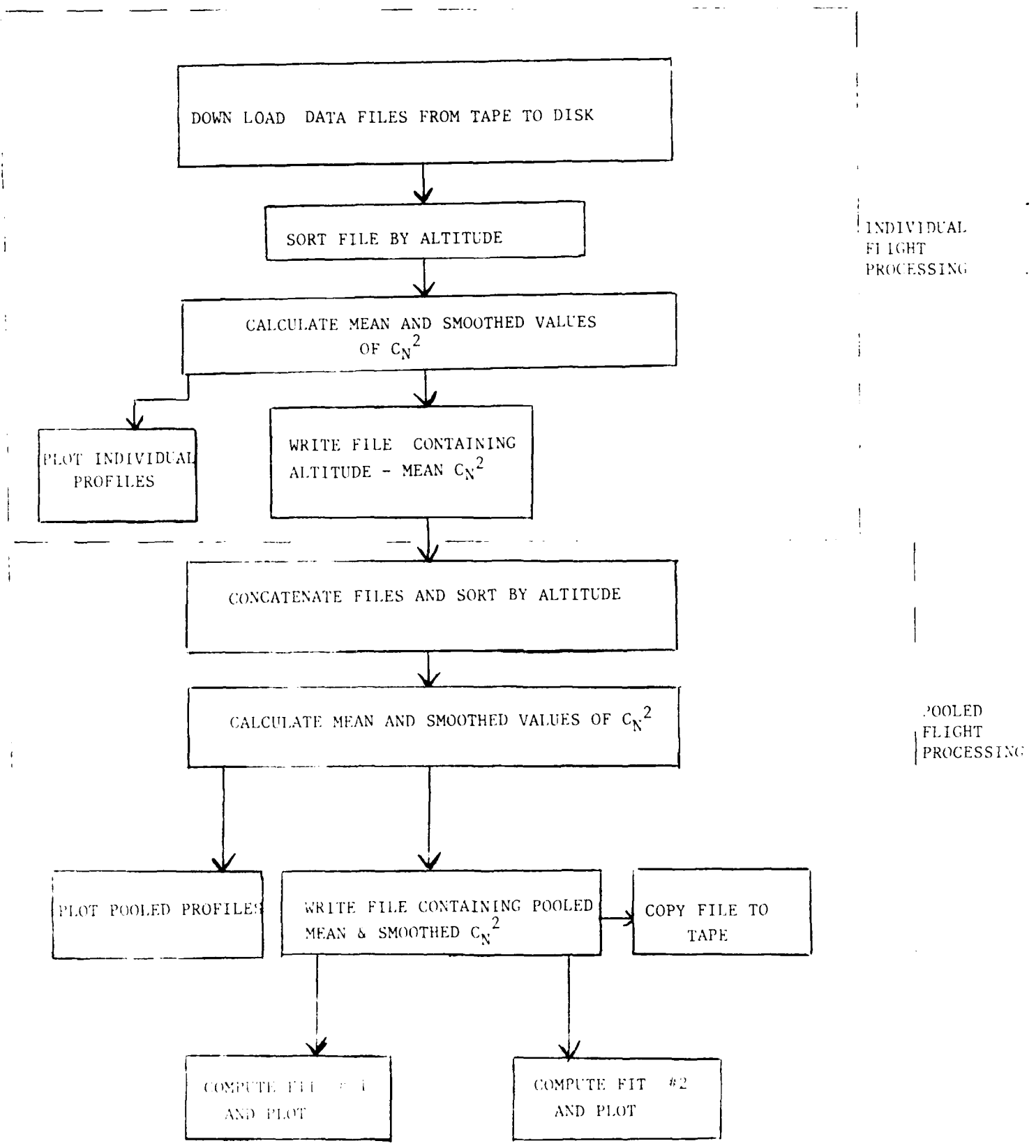


FIGURE 2.3.1 : FLOW CHART OF ADP OPERATIONS

2.3.1.3 Output

The results of individual flight operations were either plotted or stored on disk for further analysis. Plots were generated for the 3 day and 6 night flights first using a window of 20 m and then for 40 m. Thus, a total of 18 plots were created from the individual flight data.

Files containing the flight numbers, altitudes, and mean and smoothed C_n^2 scores were also produced at this stage of the analysis. These files were then concatenated into one day and one night file from which pooled mean and smoothed C_n^2 measures were constructed.

2.3.2 Pooled Flight Operations

2.3.2.1 Inputs

The concatenated files of day and night flights were used as inputs to the pooled flight program. The file description is presented in Section 2.4.

2.3.2.2 Processing

The concatenated files were sorted by altitude in ascending order and then passed through the same data checks that were performed on the individual data files. Once the integrity of the observations had been tested, they were passed into an algorithm that computed the pooled mean C_n^2 value from the individual mean scores. The pooled mean values were stored and used as inputs for the next algorithm that computed a gaussian smoothing of these values. The pooled mean C_n^2 values were also entered into a log quadratic and nonlinear equation.

The mean and smoothed C_n^2 values were created twice. The first time a standard deviation of 20 was used and the second time a standard deviation of 40 was employed.

2.3.2.3 Output

The products of the pooled processing were either plotted or stored on disk/tape files. Three plots were generated with altitude assigned to the Y-axis and the corresponding C_n^2 value on the X-axis. The C_n^2 measure was derived from either the gaussian smoothing, log quadratic, or non-linear computations. These plots were each created from the files computed with a window of 20 or 40.

Output files are written at the end of data processing. The two files generated contained the altitude and pooled mean and gaussian smoothed C_n^2 values. The only difference between these two files is that the scores were created using different standard deviations.

2.4 Data File Characteristics

2.4.1 Magnetic Tape Files

Three day and six night files were used in this study. These files resided on an ANSI-labeled tape at 1600 bpi. The tape contained 22 files written in binary format. The structure of these files is presented in Appendix A. All files had the same record format. Each file consisted of five header records that identified the flight parameters (e.g., launch date and time) and data records that had the observations for each altitude level sampled.

2.4.2 Disk Files

Since not all of the data on the tape files were necessary for the present purposes, records were truncated when written to disk. Disk files only contained the flight number, altitude, temperature, pressure, and C_n^2 scores. However, the pooled data sets only included the altitude, mean and gaussian smoothed C_n^2 scores.

3.0 DATA ANALYSIS

3.1 Overview

This section reviews the results of the analyses conducted within this investigation. It first describes the mathematical approach used and then reviews the tasks completed.

3.2 Quantitative Methods

There were two procedures used to summarize the observations in the data files. The first one was to obtain a mean C_n^2 scores for a given window as defined below:

$$\overline{C_n^2(z_i)} = \frac{C_n^2(z_j)}{n_j}$$

where z_j represents the altitude of $C_n^2(z_j)$, z_i is the altitude of the mean $C_n^2(z_i)$ score, and n equals the number of scores that fall within the window. This sample mean denotes an unbiased estimate of the population mean.

The second procedure used to aggregate the data was a gaussian smoothing technique. This approach utilized a least-squares estimate and is expressed as follows:

$$C_n^2(z_j) = \frac{A(z_i, z_j) C_n^2(z_i)}{A(z_i, z_j)}$$

where:

$$A(z_i, z_j) = 1/\sqrt{2\pi} e^{-1/2(z_i - z_j)^2/\sigma^2}$$

The mean C_n^2 values derived from the first equation were used as inputs to the log quadratic and non-linear equation. The log quadratic formula is shown below:

$$\text{Log } C_n^2(z_i) = A + Bz_i + Cz_i^2$$

where A , B , and C are coefficients of the quadratic and z_i is the altitude of case i . z_i and z_i^2 are assumed to be orthogonal.

The nonlinear (Newton-Raphson) equation used in this investigation is represented as:

$$\text{Log } C_n^2(z_i) = A + Bz_i + Cz_i^2 + D \exp(-1/2(z_i - E/F)^2)$$

where A , B , C , D , E , and F are coefficients within the expression.

3.3 Results

3.3.1 Individual Flights

The product of the gaussian smoothing of an individual day flight are presented in Figures 3.3.1.1 and 3.3.1.2. Both figures display the logarithm of smoothed C_n^2 scores on the X-axis and their corresponding altitude levels (in km) on the Y-axis. The C_n^2 values for the first figure were computed using an altitude standard deviation of 20 m while the second figure used a standard deviation of 40 m. A series of plots were produced for different flights. Flight 2X0006 demonstrated the most C_n^2 variation. Incrementing the window from 20 to 40 m shows a pronounced effect on the profile of smoothed C_n^2 values.

The gaussian smoothing of an individual night file are shown in Figures 3.3.1.3 and 3.3.1.4. Once again the smoothed C_n^2 scores were plotted on the X-axis and the altitude on the Y-axis and the smoothed C_n^2 values were computed using either a 20 or 40 m window. The differences between the 20 and 40 m computations are noticeable. The 40 m window displays less variation in C_n^2 than the 20 m window.

3.3.2 Pooled Flights

The outputs resulting from the operations performed on the concatenated day flights are presented in Figures 3.3.2.1. Figure 3.3.2.1 displays a graph of the pooled mean C_n^2 scores by their corresponding altitudes. The graph was computed using the standard deviation of 20 m. Figure 3.3.2.2 shows the results of the gaussian smoothing of pooled mean C_n^2 night flights.

Figure 3.3.2.2 depict the pooled mean and gaussian smoothing of the pooled mean C_n^2 for the concatenated night flights having a 20 m window. From inspection of the 20 m and 40 m plots, the decision was made to only include the 20 m windowed data set in the quadratic and nonlinear fits.

The coefficient used to plot the quadratic and nonlinear fits of pooled mean C_n^2 values are shown in Table 3.3.2.1. Using the coefficients displayed in the top portion of this table, the fitted lines were estimated for the day and night flights and plotted in Figure 3.3.2.3 along with the smoothed C_n^2 lines. Similar plots were drawn using the coefficients shown at the bottom part of Table 3.3.2.1 were drawn in Figures 3.3.2.4 and 3.3.2.5. These plots represent the nonlinear fit of day and night data, respectively.

GAUSSIAN SMOOTHED CN**2
FOR DAY FLIGHT 2X0006
SIGMA = 20M

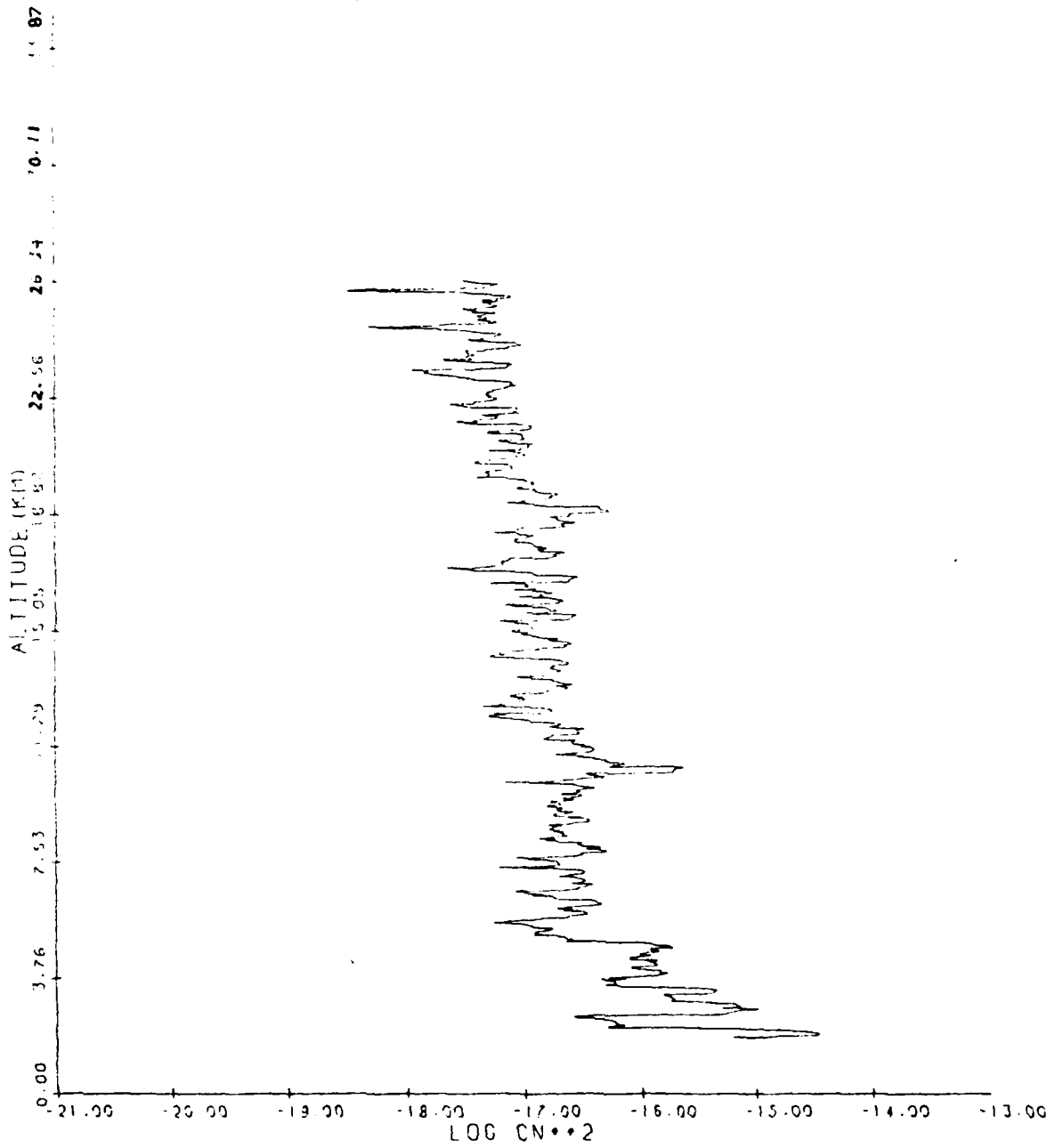


Figure 3.3.1.1

GAUSSIAN SMOOTHED CN**2
FOR DAY FLIGHT 2X0006
SIGMA = 40M

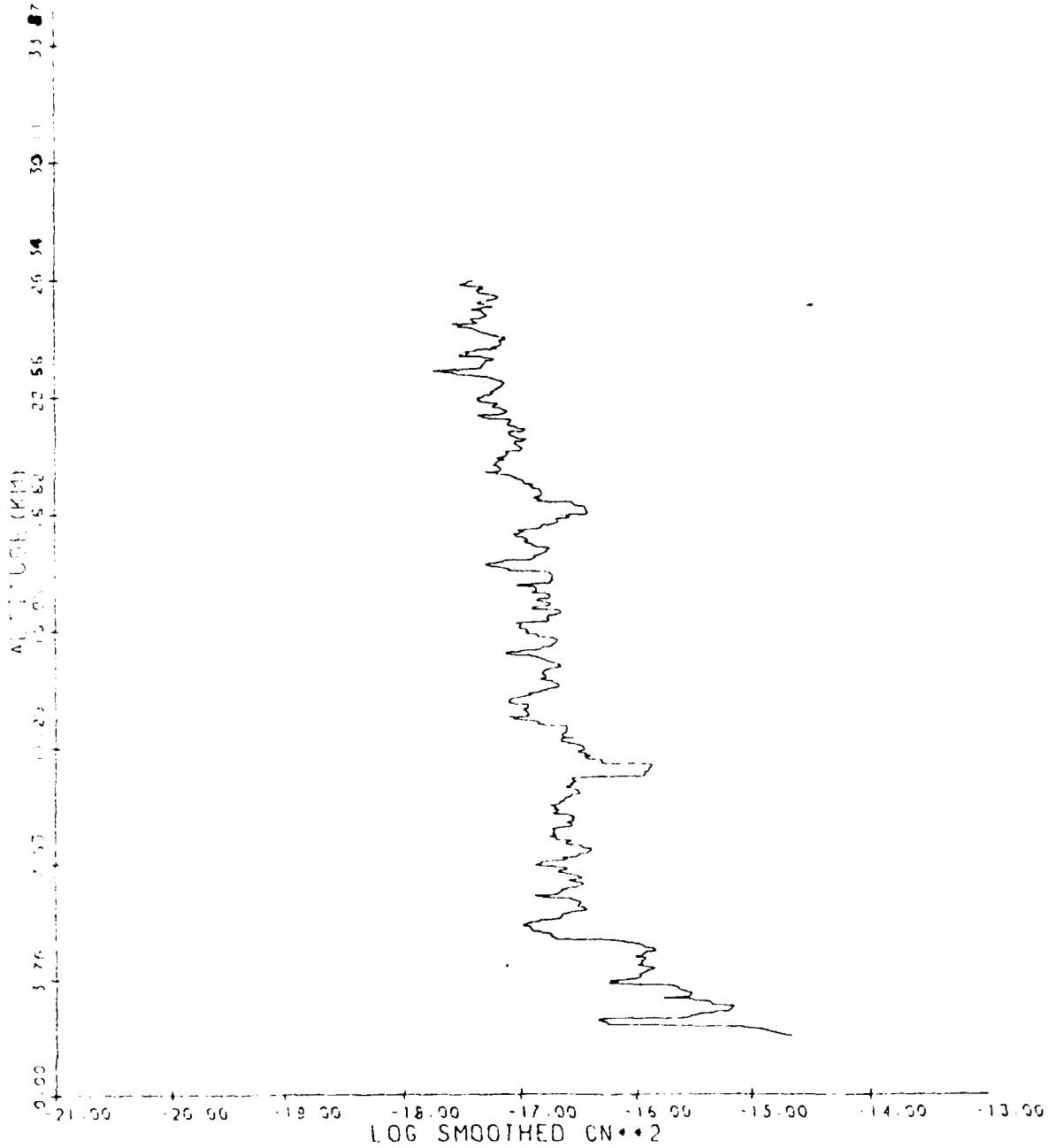


Figure 3.3.1.2

GAUSSIAN SMOOTHED CN**2
FOR FLIGHT 2X0004
SIGMA = 20M

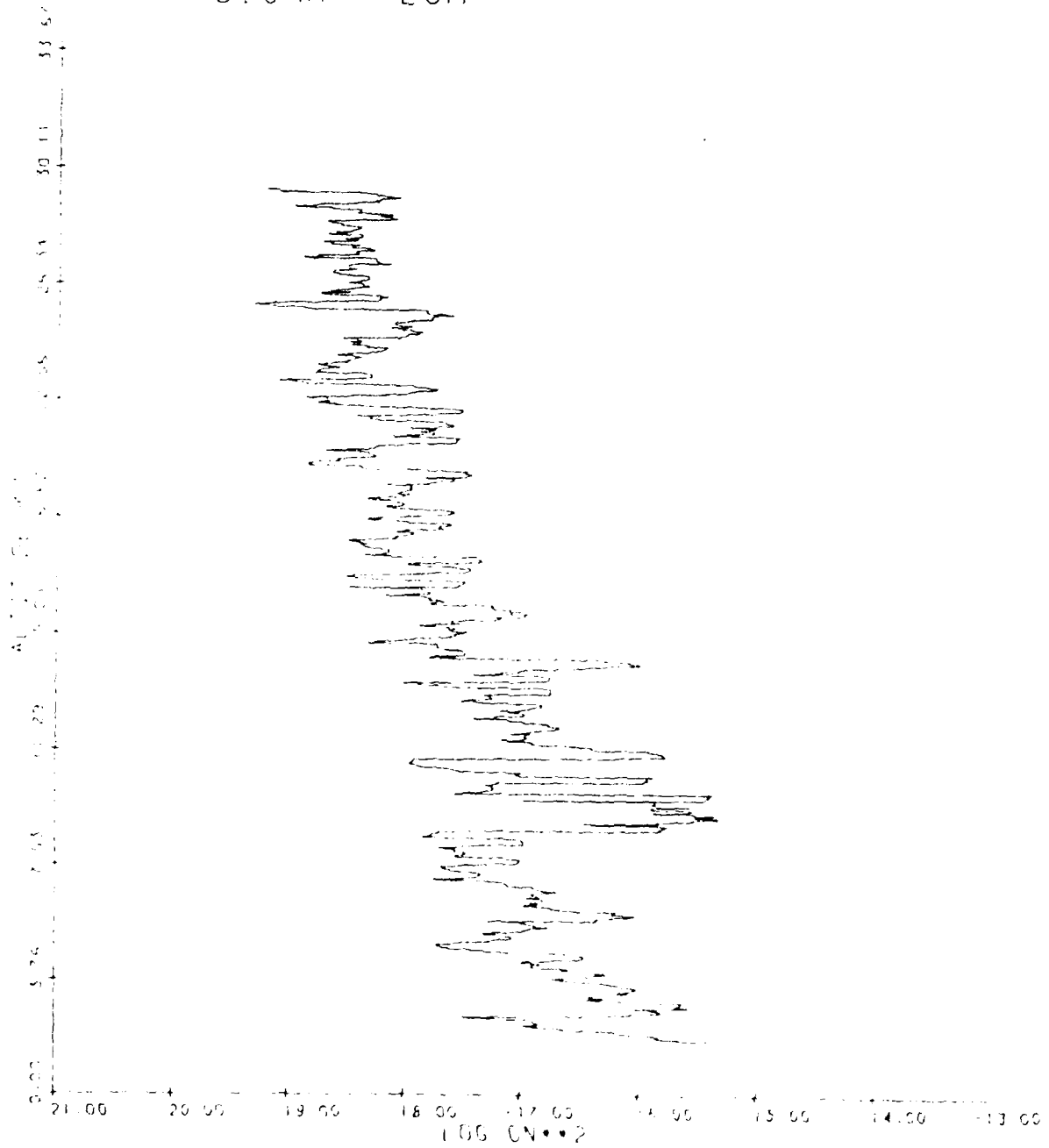


Figure 3.3.1.3

GAUSSIAN SMOOTHED CN**2
FOR FLIGHT 2X0004
SIGMA = 4CM

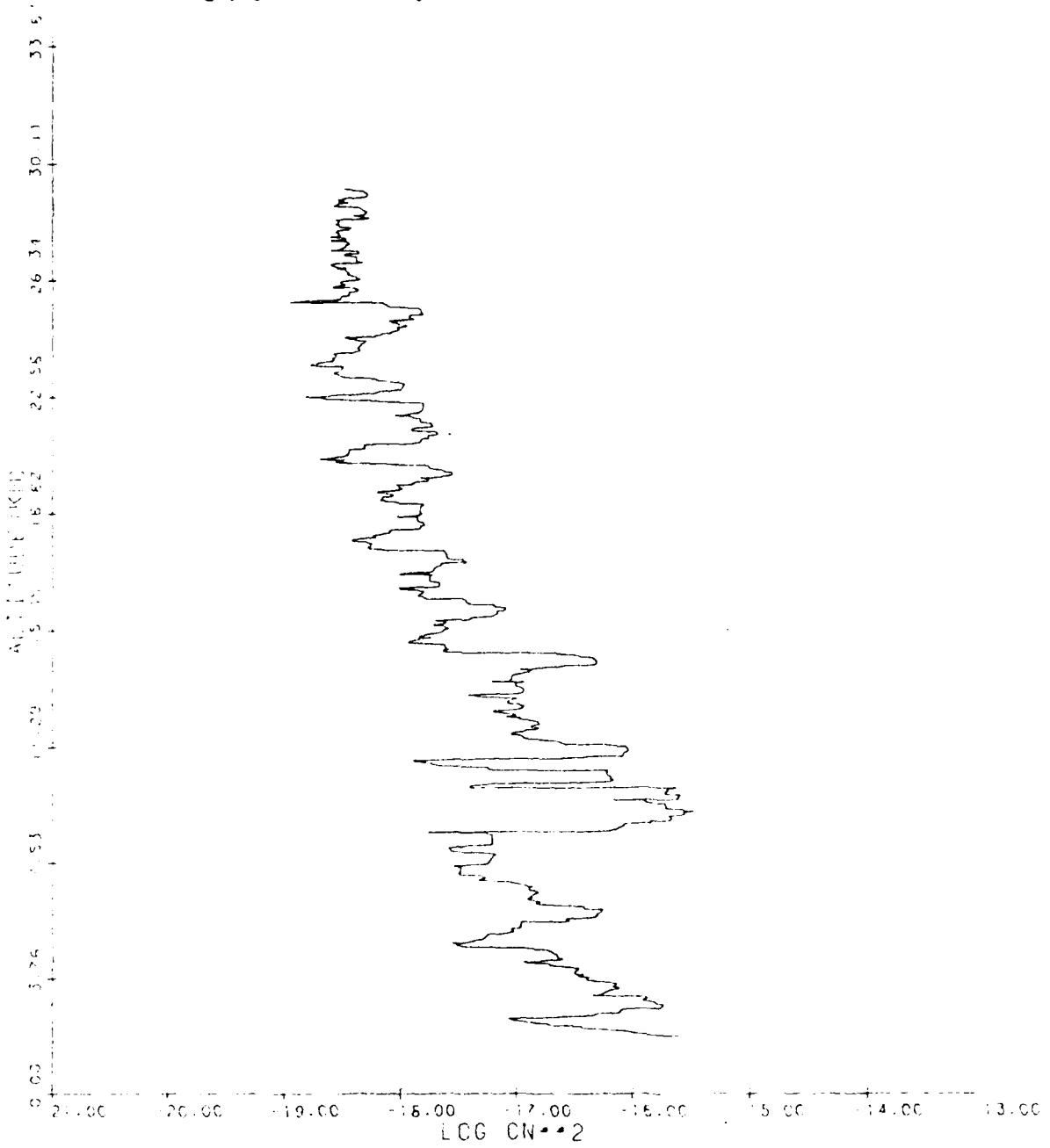


Figure 3.3.1.4

GAUSSIAN SMOOTHED CN**2
FOR 3 DAY FLIGHTS
WINDOW = 20M

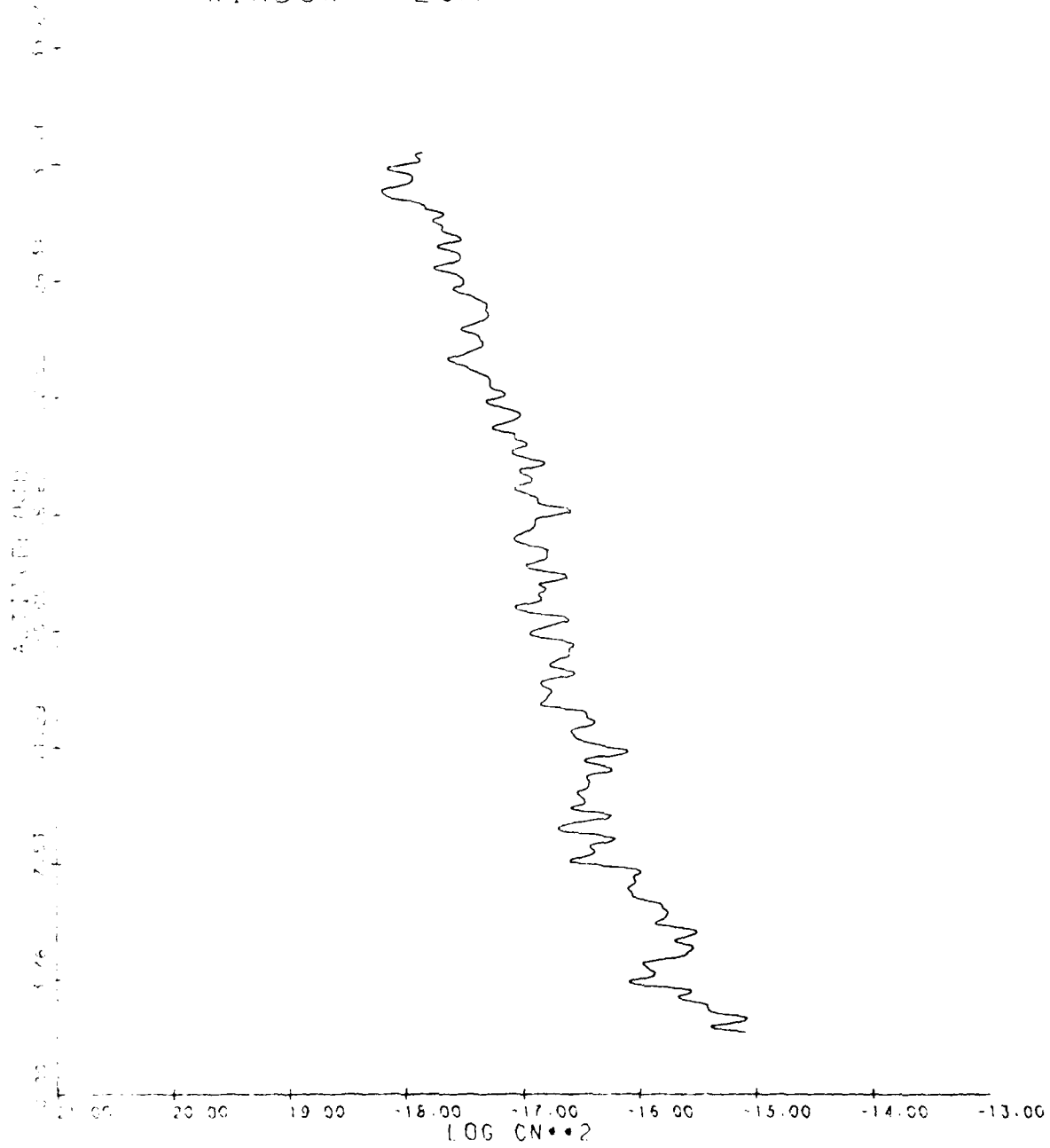


Figure 3.3.2.1

GAUSSIAN SMOOTHED CN**2
FOR 6 NIGHT FLIGHTS
WINDOW = 20M

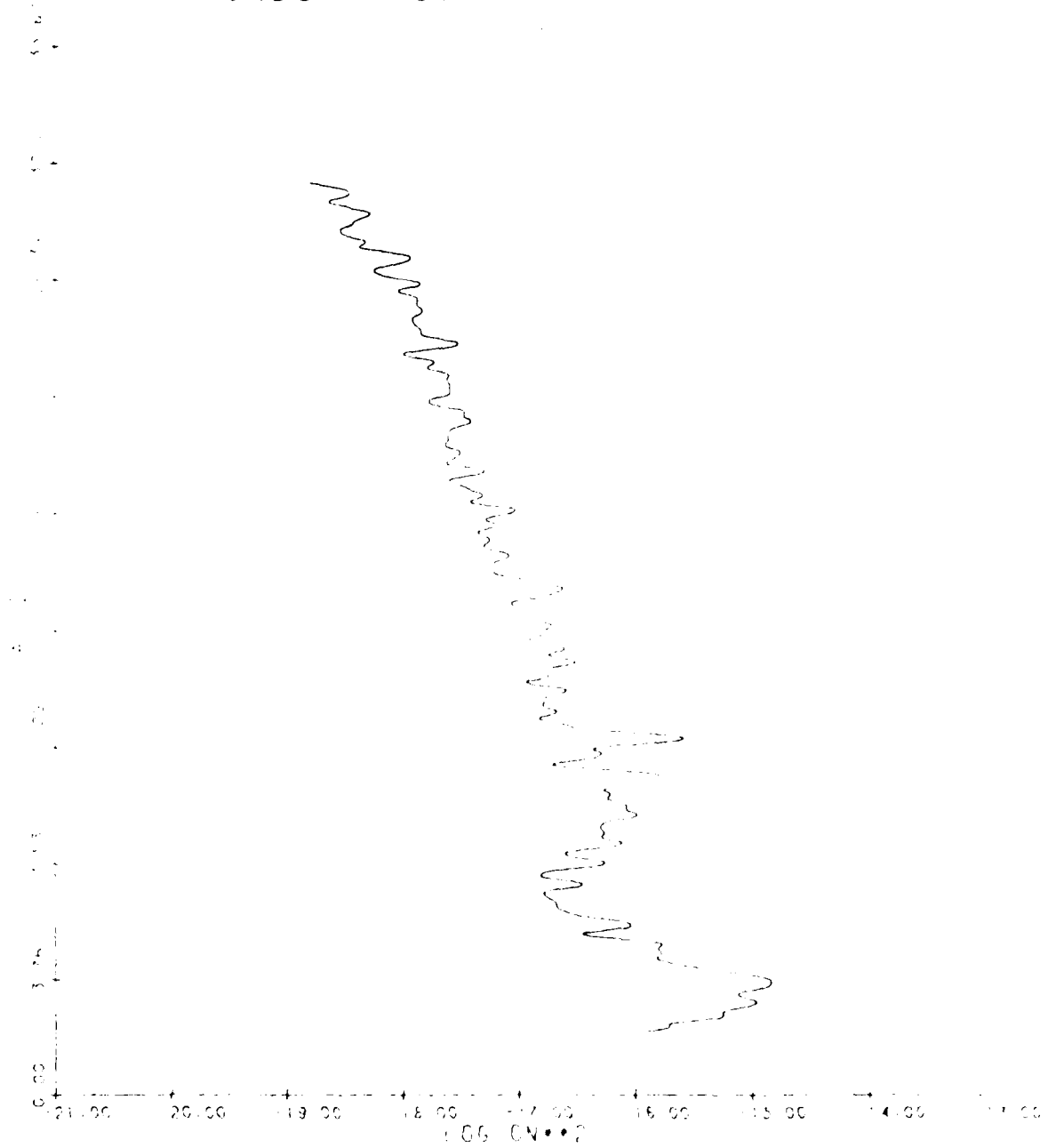
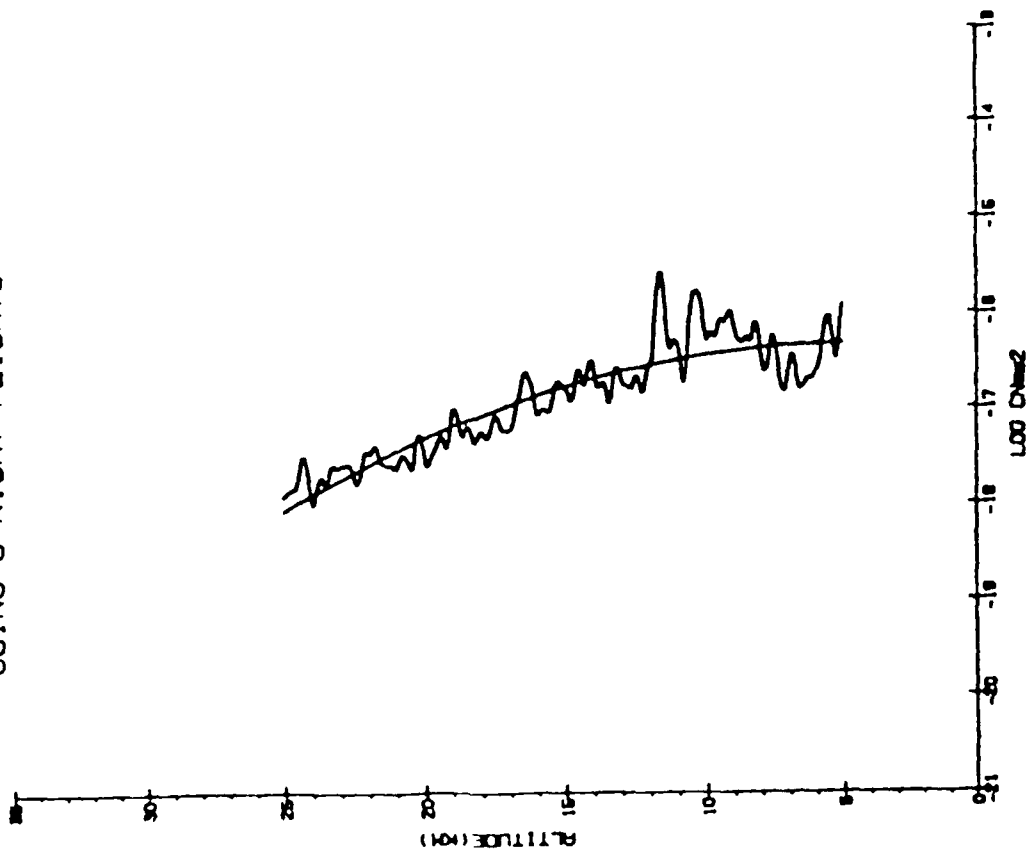


Figure 3.3.2.2

QUADRATIC FIT OF
SMOOTHED $CN_{\text{M}2}$ SCORES
USING 6 NIGHT FLIGHTS



QUADRATIC FIT OF
SMOOTHED $CN_{\text{M}2}$ SCORES
USING 3 DAY FLIGHTS

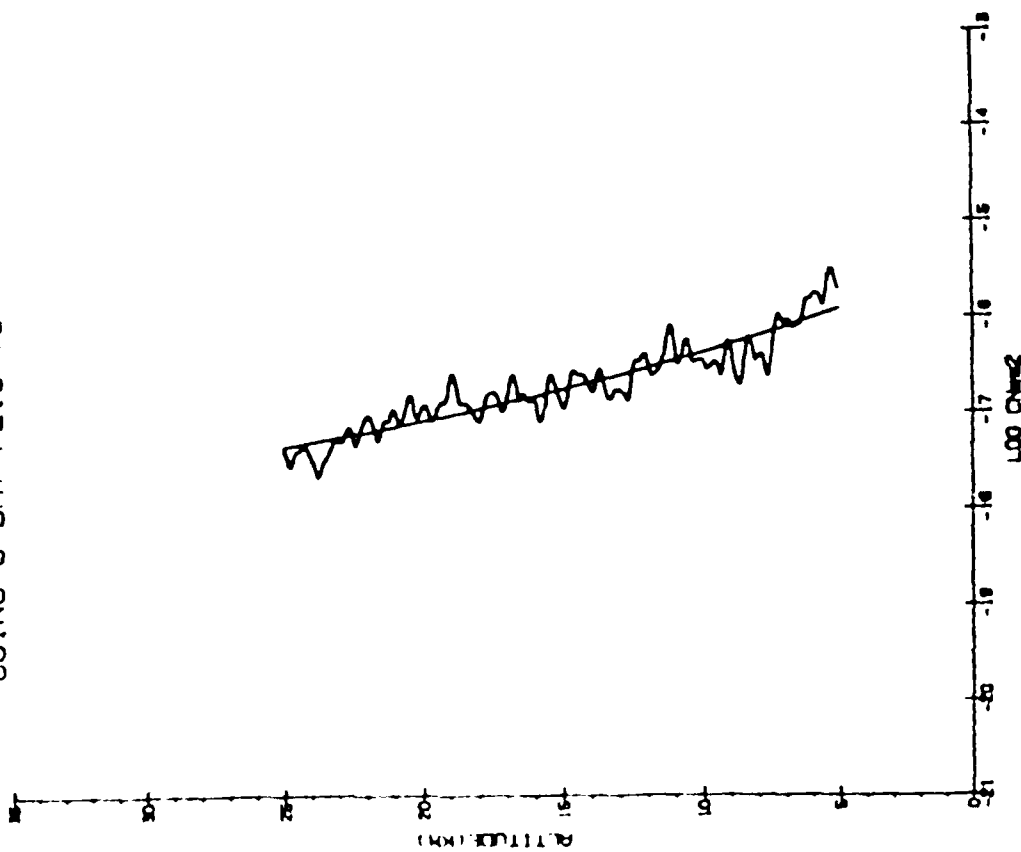


Figure 3.3.2.3

NONLINEAR FIT OF
SMOOTHED CN**2 SCORES
USING 3 DAY FLIGHTS

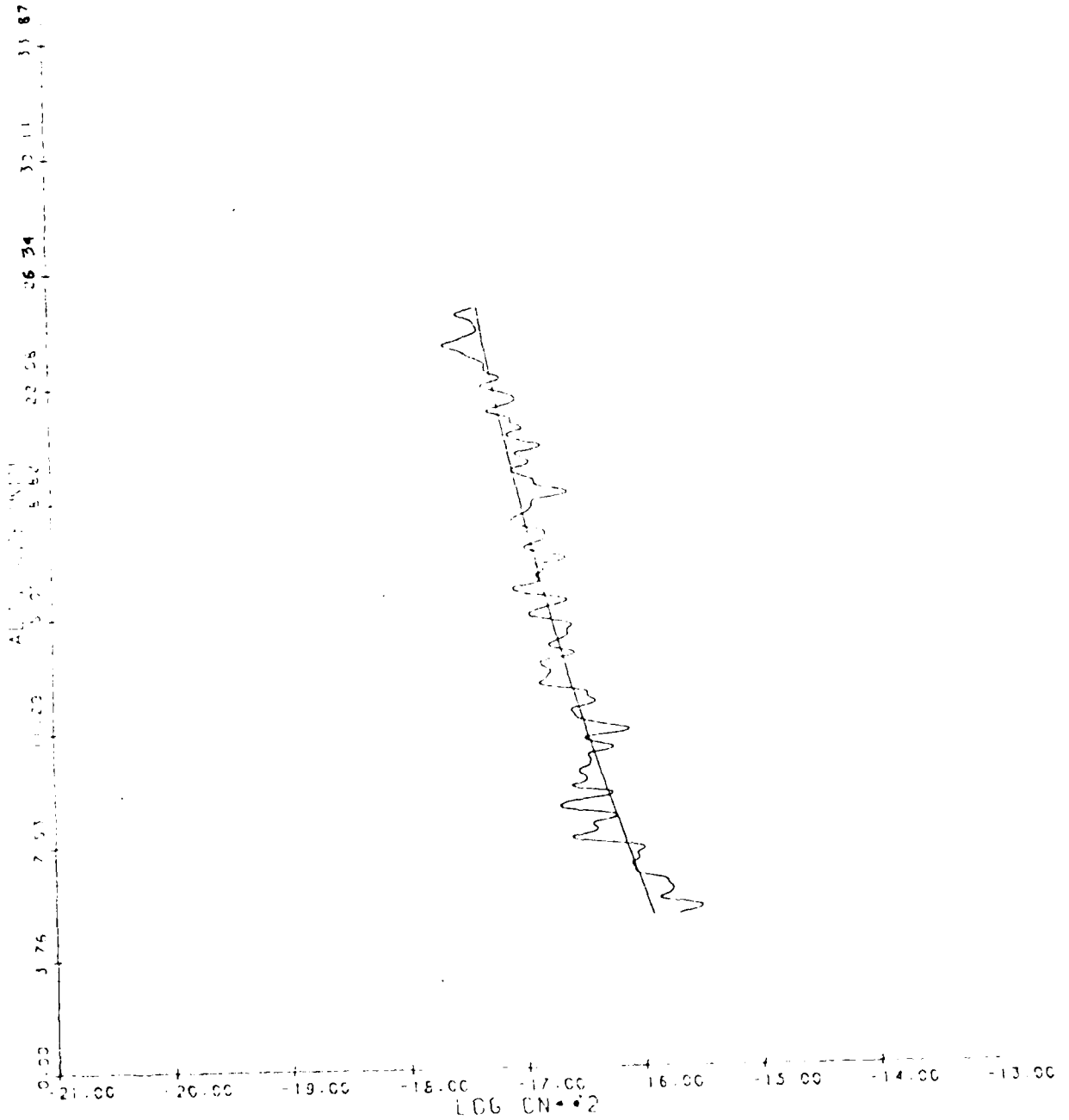


Figure 3.3.2.4

NONLINEAR FIT OF
SMOOTHED CN**2 SCORES
USING 6 NIGHT FLIGHTS

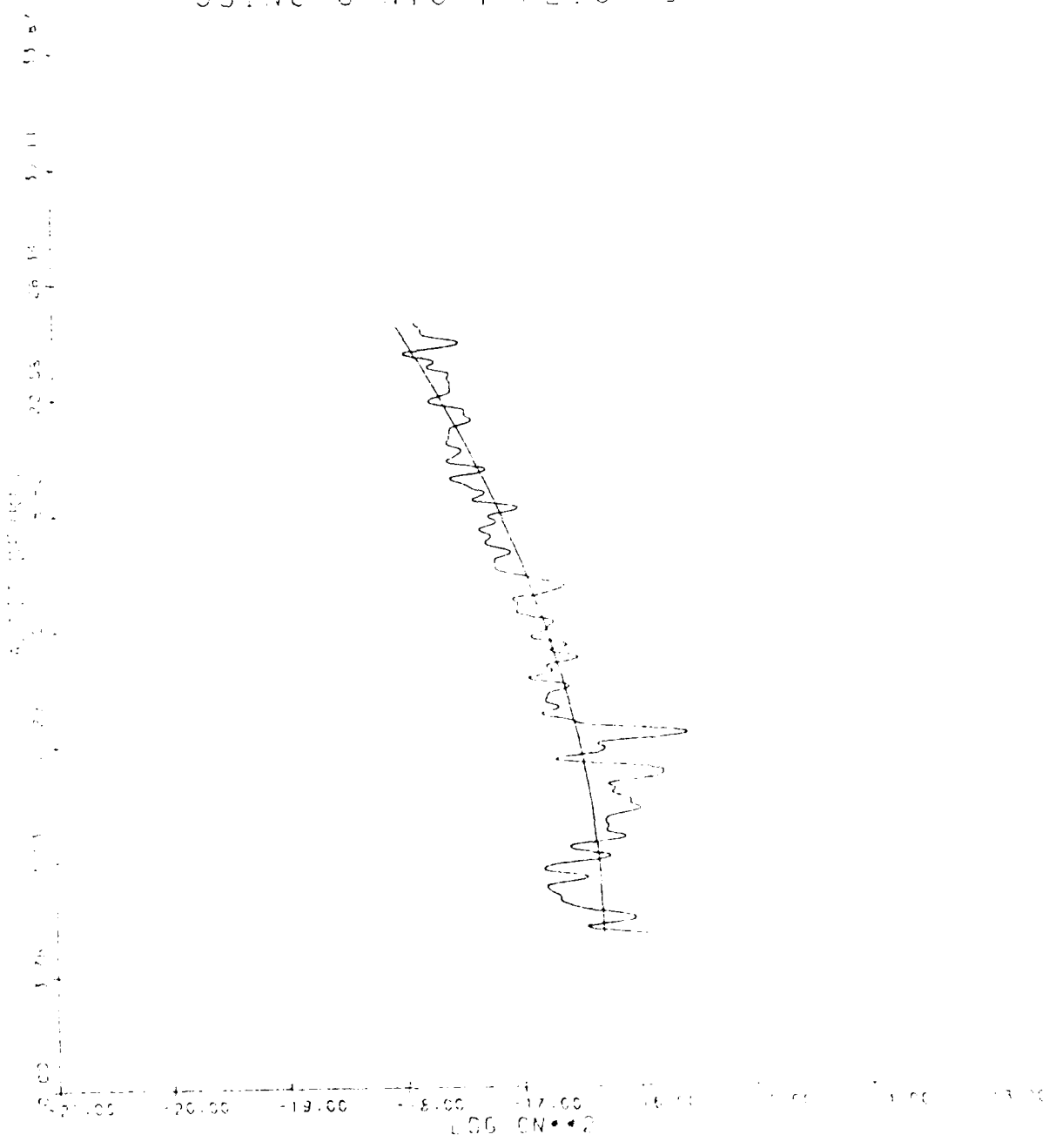


Figure 3.3.2.5

Table 3.3.2.1

Table of Coefficients Used in
Quadratic and Non-Linear Fits

		Coefficients	
<u>Fit</u>	<u>Label</u>	<u>Day</u>	<u>Night</u>
Quadratic:	A	.27098204164081E-15	.66403310568815E-16
	B	-.29345519050923E-16	-.13270127983623E-17
	C	.78936744783121E-18	.77160351583446E-19
Nonlinear:	A	-.773795E+2	-.763804E+2
	B	.152222	-.434465E-2
	C	.128323E-2	-.418050E-2
	D	.544582E+5	.528689E+5
	E	.199407E+5	.195242E+5
	F	.541586E+4	.530145E+4

APPENDIX A

Data Format of Mag Tape File:
VSN = CC4459

<u>Word Number</u>	<u>Content</u>	<u>Format</u>
	<u>Header No 1:</u>	
1	Name	A10
2	Launch date	A10
3	Launch time	F10.2
4	Reference	F10.2
5	Minimum Frequency	F10.2
6	Maximum Frequency	F10.2
7	Run Date	A10
	<u>Header No 2:</u>	
1	R ₀	F10.2
2	R ₃₀	F10.2
3	R ₃₃	F10.2
4	T _{wet}	F10.2
5	T _{dry}	F10.2
6	P ₀	F10.2
7	R ₁₀	F10.2
8	A ₀	F10.2
9	Run Date	A10
10	# Words/Record	I10
	<u>Header No 3:</u>	
1	Thermosonde	I1
	<u>Header No 4:</u>	
1	# words following low gain	I4
2	1st time division	F10.2
3	1st thermosonde correlation	F10.2
4	2nd time division	F10.2
5	2nd thermosonde correlation	F10.2
	— Repeats for # words specified in word 1 —	
	<u>Header No 5:</u>	
1	# words following high gain	I4
2	1st time division	I4
3	1st thermosonde correlation	F10.2
4	2nd time division	F10.2
5	2nd thermosonde correlation	F10.2

APPENDIX A (continued)

Data Record:

1	Record Number
2	Time
3	Frequency Reference
4	CINT
5	Temperature (C°)
6	C. Temperature
7	CH
8	C CH

Contents:

9	Altitude
10	C. Altitude
11	Frequency pressure
12	KLASS
13	IPRESS
14	Pressure
15	Frequency - (Thermo-low)
16	Thermosonde CT
17	C_N^2
18	Frequency (Thermo-high)
19	Thermo CT
20	C_N^2
21	C_N^2 combined
22	Altitude
23	Position East
24	Position North
25	Vel. East
26	Vel. North
27	Vel. Vertical
28	Vel. Horizontal
29	SHOR
30	Smoothed C_N^2
31	Sigma C_N^2
32	NIOT

TURBOPAUSE HEIGHT STUDY

1.0 INTRODUCTION

The purpose of this study was to determine if a relationship exists between turbopause height and solar flux (measured by $F_{10.7}$).

2.0 DATA PROCESSING

2.1 Data Description

Fifteen years of rocket data were collected from two stations: Eglin AFB and Heiss Island. Variables recorded included date, local time, and turbopause height. A_p , K_p , and $F_{10.7}$ measurements have been integrated into the data set using the time and data information.

2.2 Data Analysis

2.2.1 Overview

Raw data was inspected for outliers using scatter diagrams of turbopause height and other variables. Some data records were removed if inaccurate, or alternatively the turbopause height was adjusted. K_p values were also corrected as necessary. A final collection of 70 records were deemed valid for further consideration.

The data was split into seasons, defined as follows:

Winter	—	Dec 1 - Mar 15	26 records
Spring/Summer	—	Mar 16 - Sep 15	25 records
Fall	—	Sep 16 - Nov 30	19 records

2.2.2 Fall Data

The fall data was removed from further analysis due to its lack of significance in determining a relationship between solar flux and turbopause height. This was determined by the Initiator from previous work on the fall data.

Initial descriptive statistics (means, variances, and correlation matrices) of the winter and spring/summer data sets were done on all the variables. For the sake of completeness, the fall data was included in this preliminary analysis.

2.2.3 Winter Data

A descriptive statistics analysis was done to examine the characteristics of the winter data set. Significant correlation coefficients were observed in the correlation matrix. They are tabulated as follows:

Turbopause Height with K_{p1}	.4157
A_{p3} with K_{p1}	.7731
K_{p2} and $F_{10.7}$	-.4569

A stepwise multiple regression of the winter data was done. The K_{p1} variable entered the regression equation at a .05 level of significance. The resulting equation:

$$\text{Turb. Ht.} = 105.42 + 1.5(K_{p1})$$

has a multiple correlation coefficient of .173, which is not a highly significant model result.

2.2.4 Spring/Summer Data

The original data set of spring/summer was examined. The descriptive statistics along with a set of scatter diagrams are presented. There were no significant relationships present between any of the variables in the correlation matrix of the spring/summer data set. A stepwise multiple regression analysis was performed and, likewise, no variables were entered into the model to estimate the turbopause height.

2.2.5 Diurnally Corrected Data

For the winter and spring/summer data sets, a diurnal component was detected after examination of local time vs. turbopause height plots. The diurnal variation of each season was removed and a summary statistics analysis was performed.

Similar results to those in 2.2.3 were found in the diurnally corrected winter data. That is, K_{p1} had a high enough correlation (at the .05 level) to be included in a stepwise regression model. The correlation coefficient between turbopause height and K_{p1} was .3889. The resulting equation:

$$\text{Turb. Ht.} = -2.19 + 1.22(K_{p1})$$

has a multiple correlation coefficient of .151, which is not a highly significant model result.

The diurnally corrected spring/summer data had no statistically significant characteristics for accessing the relationship between solar flux and turbopause height, but the scatter plot of $F_{10.7}$ and turbopause height revealed an interesting structure.

2.2.6 Yearly Averaged Data

Yearly turbopause height values were averaged for each season. Descriptive statistics and scatter diagrams were utilized to determine if any relationship existed between turbopause height and solar flux ($F_{10.7}$). A hand drawn curve was placed over the turbopause height vs $F_{10.7}$ graph to examine the trend that turbopause height had with time. A basic pattern developed: in winter a counter clockwise rotation of turbopause height was seen through time, and in the spring/summer a general clockwise rotation was seen through time.

2.2.7 Station Split Data

The spring/summer and winter data was split into each station: Eglin AFB and Heiss Island. A similar hand drawn curve was overlaid onto the turbopause height vs $F_{10.7}$ graphs to examine the flow of turbopause height in relation to solar flux through time. Due to the scarcity of data in each station's season, (n=9,12,13, or 17) a vague ellipse is evident showing:

Winter - counter clockwise rotation of turbopause height in relation to solar flux through time

Spring/Summer - clockwise rotation of turbopause height in relation to solar flux through time.

3.0 SUMMARY

A basic relationship between turbopause height and the solar rotational effect has been determined. Even though the data set had been scarcely and inconsistently gathered throughout time (70 valid records over 15 years), a distinct trend in the direction of turbopause height in relation to solar flux through time was evident. It is understood that there was great expense in gathering each record, which consisted of a rocket launch.

The relationship between turbopause height and the solar rotation cannot be described by a formal statistical model due to the nature of the data set as mentioned in the previous paragraph. However, again stated, the following relationship did appear founded. Given diurnally corrected and yearly averaged turbopause height values, as well as a solar flux indicator ($F_{10.7}$), the following relationships were noted:

(1) There is evidence of a counter-clockwise rotation of the turbopause height in relation to the solar rotation during the winter (defined from December 1st through March 15th) season.

(2) Similarly, there is evidence of a clockwise rotation of the turbopause height during in relation to the solar rotation during the spring/summer (defined from March 16th to September 15th) season.

It is evident that more data must be gathered in order to substantiate this claim.

INSTANTANEOUS RAINFALL ANALYSIS

1.0 INTRODUCTION

1.1 Overview

This report summarizes the technical and analytical support provided by Bedford Research Associates (BRA) to the Design Climatology Program which is directed by the Tropospheric Structure Branch of the Air Force Geophysics Laboratory (AFGL) located at Hanscom Air Force Base, Bedford, MA. It describes the ADP software and analyses used to evaluate the parameters of intense rainfall.

1.2 Background

The Design Climatology Program develops techniques for incorporating climatic information into the design, operation, and evaluation of aerospace equipment. One method under current investigation is the statistical modeling of 1-minute rainfall rates. The study of rainfall is significant because rain can disrupt normal Air Force operations in many ways. For example, heavy intensities of precipitation attenuate the microwave signals transmitted by radar systems for satellite detection and tracking, surveillance, and reconnaissance. Rainfall also adversely affects the operation of aircraft through erosion of leading edges (e.g., helicopter blades) or malfunction of jet engines. Therefore, a better understanding of the characteristics of rainfall rates will enhance the design and function of Air Force systems.

Despite the significance of this atmospheric event on aerospace systems, there exists little empirical data on the characteristics of 1-minute, instantaneous rainfall rates. Tattelman and Grantham (1982) have reviewed the literature and concluded that estimates of instantaneous rainfall are restricted by inherent methodological weaknesses. Specifically, errors in data collection, caused by inaccurate measuring devices and large annual variations in the rainfall distribution raise questions about the validity of previous findings. The only technique for developing an accurate model of instantaneous rainfall is to compile a data base containing continuous and reliable measurements for at least 5 years. This strategy should

compensate for the experimental error resulting from poor instrumentation and yearly variations.

1.3 Objectives

The primary objective of this investigation was to evaluate the frequency and duration of 1-minute rainfall rates compiled over a 10 year period. This study assessed the annual, monthly, and seasonal patterns of rain in order to develop a more comprehensive understanding of its properties. More specifically, the tasks conducted under this project were to:

- * Examine the contents of the tape files to determine the integrity of the data.
- * Identify rainfall rates ranging between .001 and 10.5 mm/min and count the frequency of occurrence at various intervals and durations.
- * Aggregate the rainfall by annual, monthly, or seasonal groups and plot the frequency distribution for various durations.
- * Investigate the number of times that the rainfall duration crossed seasonal boundaries.
- * For each season within the 10 year span, determine the longest duration of rainfall with rates between .1 and 2.5 mm/min and report the year and length of that duration by season and threshold value.
- * Repeat the above analysis for each of the months within the data file and report the results by months instead of seasons.
- * Calculate and plot the Poisson probability distribution of seasonal rainfall for varying duration and thresholds.
- * Explore the relationship between the rainfall intensities and duration lengths and tabulate the findings.
- * Tabulate the rainfall rates at thresholds ranging from .001 to 2.5 mm/min by the season and hour of the day.
- * Group the data by 4-hour intervals and plot the frequency distribution for different thresholds and seasons.
- * Refine the output generated from the above analyses for final delivery.

The ultimate goals were to establish a more comprehensive explanation of the properties of instantaneous rainfall and to develop software that could

be used to replicate these analyses on other rainfall data bases.

1.4 Methodology

This project was partitioned into four distinct phases. The first phase involved determining the structure and content of the data sets. All relevant magnetic tapes and documentation were reviewed to insure the integrity of the elements with the file. Programs were also run to identify the file characteristics. Once the data was verified, the second phase, establishing software requirements, commenced. During this process, the specific statistical analyses were identified. The data to be analyzed (e.g., intensity, duration) and the form of the output (e.g., tables or plots) were defined. Based on these specifications, the routines were written and placed within the main program. The final phase involved reviewing the results to determine the subsequent analyses.

1.5 Report Organization

The remainder of this report describes the software development and data analyses used in the rainfall project. In the next section, the main program and data files are presented. The operations performed by the main program and the characteristics of the rainfall files are discussed. The subsequent section explains the data analyses performed under this project. The final section provides a summary of the results and considerations for future research in the area of instantaneous rainfall.

2.0 SOFTWARE SYSTEM

2.1 Overview

This section presents a functional description of the software written to evaluate the rainfall data files. It identifies the inputs, processing, and outputs of the main program used in this investigation. In addition, it outlines the format and structure of the data files. The purpose of this section is to identify the major ADP components of this project.

2.2 Environment

2.2.1 Hardware

All ADP work was performed on the AFGL Control Data Corporation (CDC) Cyber mainframe. This system had a 170/750 processor with 262K words of primary memory. It accessed 14 disk drives for a total storage capacity of approximately .5M words. Also, there were 11 tape drives (mixed 7- and 9-track) that handled tape densities between 556 and 6250 bpis. Four line printers (3 1200 lpm or 1 Xerox page printer) and a Calcomp 1055 drum plotter were available to generate output from the system.

2.2.2 Software

The Cyber mainframe ran under the NOS 2.3 operating system. It supported a variety of software needed for text editing, file manipulation, and data analysis. The Interactive Facility (IAF) was used to access the XEDIT text editor that created and modified program files. The source code for the main program was written in ANSI standard Fortran (Extended Version 4.7 or 5.0). Programs were also written in NOS command language to perform file maintenance. Fortran and AFGL Plotting libraries were used to plot the results.

2.3 Program Description

The main program developed for the rainfall analysis was written in Fortran 5.0 and stored on-line in a indirect access file and off-line on a backup tape. The remainder of this section explains the operations performed by the main program.

2.3.1 Inputs

Inputs were obtained from two sources. The first source was from within the batch file. These inputs defined the parameters of that run. These parameters included identification of the plotting profile (linear, semi-linear, or logarithmic), definition of the X-axis origin for plotting, determination of the number of duration intervals and time span (e.g.,

seasonal, monthly, or annual) used in the computation.

The second source of input was the 1-minute rainfall data files. Two direct access files contained rainfall measures sampled at 1-minute intervals for a combined total of over 10 years. These two files were sequentially attached to the main routine each time it was run. (A more detailed description of the contents of these files is presented in Section 2.4).

2.3.2 Processing

Meetings were held to obtain the requirements for each analysis. At these meetings, the specific time frame, durations, and threshold levels were specified. The type of computation and form of the output were also decided. The input parameters to the main program were then modified and adjustments to the subroutines were made to provide the requested computations and results. As each record was read from the data file, it passed through a series of data checks. Records were excluded if they were not collected at the Illinois station, were coded as bad data, or were taken after the last date on the preceding tape. Cases were also flagged if they contained rainfall durations that crossed seasonal boundaries.

Once the data had filtered through these checks, it became part of the sanitized data set used in the data analysis. The statistics routinely computed on this file were:

- * number of years included in the analysis
- * number of consecutive minutes that pre-determined time intervals or threshold levels were exceeded
- * maximum duration rate
- * average frequency count by season, month, or year
- * converting scores to logarithmic scale
- * plotting the defined profile
- * writing the results to a separate file for future analysis

The results of each analysis were used to formulate the specifications of the next step in the evaluation process.

2.3.3 Output

At the completion of each run, the results were summarized in tabular and/or graphic form. The objective was to depict the output in a way that highlighted the salient features. The statistics were either routed to a printer/plotter or stored on a disk file for future reference.

A list of plots and tables generated by the software is presented below:

PLOTS:

Seasonal:

- * overlaid frequency plots of 1, 5, 10, 15, 20, and 30 minute durations for up to 1 mm/min or 2.5 mm/min.
- * probability (Poisson) of 1, 3, 5, 10, 15, and 20 minute durations up to 1.0, or 2.5, mm/min.
- * hourly interval (0-4, 4-8, 8-12, 12-16, 16-20, 20-24) overlaid on 1, 5, 10, 15, 20, and 30 minute durations for up to 2.0 mm/min.

Monthly:

- * overlaid frequency plots of 1, 5, 10, 15, 20, and 30 minute durations for up to 1 mm/minute.

Annual:

- * overlaid frequency plots of 1, 5, 10, 15, 20, and 30 minute durations up to 1 mm/minute.

TABLES:

Seasonal:

- * frequency and average intensity of rainfall for duration lengths ranging from 1 to 1440 minutes.
- * year and longest duration for thresholds of .1, .2, .3, .4, .5, .6, .7, .8, .9, 1.0, 1.3, 1.6, 2.0, and 2.5 mm/minute
- * frequency distribution of 1 minute rainfall rates by time of day (in hours) for varying threshold levels.
- * frequency of rainfall rates by hourly intervals for rates of .001, .25, .50, .75, 1.0, 1.5, and 2.0 mm/minute and rainfall durations of 1, 5, 10, 15, 20, 30, and 35 minutes.

Monthly:

* year and longest duration for thresholds .1, .2, .3, .4, .5, .6, .7, .8, .9, 1.0, and 2.5 mm/min.

Seasonal

Monthly

Annual:

* frequency distribution of 1, 5, 10, 15, 20, 25, 30, and 35 min durations for varying thresholds from .01 to 10.

2.4 Data File Description

2.4.1 Magnetic Tape Files

The Illinois data resided on two magnetic tapes. These tapes were both internally unlabeled and written in fixed block formats. The first tape, TN=KRAIN1, contained 35.5 months of Illinois rainfall data recorded between May 1969 and April 1972. The second tape, TN=RAIN1, had 92 months of Illinois data collected from January 1972 to August 1979. A copy of each file was created on disk. Appendix A contains a more detailed description of the tape characteristics.

2.4.2 Record Format

Appendix B and C contains the format of the KRAIN1 and RAIN1 data files, respectively. Inspection of these files will reveal that the first seven fields in both files were identical. The first field was coded to either indicate the beginning/end of the file or the integrity of the data within that record. The second field identified the station where the data had been recorded and the third through seventh field showed the year, month, day, hour, and minute that the data was recorded. The remaining fields on each record were used to record the rainfall rates to the nearest .001 mm. The KRAIN1 file contained 60 1-minute measures of rainfall on each record while the RAIN1 file consisted of 15 1-minute rainfall recordings.

3.0 DATA ANALYSIS

3.1 Overview

This section discusses the evaluation process undertaken in this investigation. It is divided into two parts. The first part reviews the descriptive statistics collected on the entire data set. The second part reports the annual, monthly, and seasonal breakdown of the file. The rationale for each analysis and a synopsis of the results are presented.

3.2 Descriptive Statistics

The first steps taken in this analysis were to confirm the general features of the data. Using the supporting documentation provided with the tapes and published information about the data base, a series of descriptive statistics were developed to verify the data. From these analyses, it was determined that the file contained 5,256,000 1-minute rainfall rates that spanned over a ten year period. The beginning and end dates were May 1, 1969 and August 31, 1979, respectively. Unfortunately, May fell in the middle of spring and inclusion of the May 1969 data would have artificially distort the seasonal statistics. To resolve this problem, the May 1969 month was removed from any analyses. The station identification number was then examined to insure that all recordings were collected at the Illinois location. A missing case report was also performed to determine the amount of lost information. This report revealed that approximately 109 records or 0.5% of the observations were unusable.

The next step was to examine the frequency distribution of rainfall rates between .001 and 10 mm/min. The results of this analysis are presented in Appendix D. Inspection of this table will show that the increment between various rainfall rates differed. For rain frequencies between .001 and 1.0, the gradient is .01 whereas this value increases to .1, .5, or 1.0 with higher intensities. Since the majority of rates occurred between .001 and 1.0, this strategy was used to discriminate between sampling points. Rainfall occurrence was most frequent between .001 and 0.5 mm/min (169108 observations in 10.25 years). Rains intensities drop off by more than one

order of magnitude in the bin interval .05 to .10 mm/min (24069 observations) and interval .10 to .15 mm/min contains 7197 observations, after which there is a gradual linear decline in observations.

3.3 Annual, Monthly, and Seasonal Analyses

The results of the previous analyses identified the global characteristics of the data. To obtain a better understanding to the trends that existed, the focus of analyses turned toward annual, monthly, and seasonal profiles. Rain intensities between 0.1 and 1.0 mm/min (or 2.5 mm/min) with durations of 1, 5, 10, 15, 20, and 30 minutes were evaluated. Initially the intensity plots were broken down by annual, monthly, or seasonal divisions. There is little empirical information available to predict the yearly or monthly trend of rainfall although previous research has found the greatest rates of precipitation in summer and the least in the winter. The outcome of the seasonal analysis supported these earlier findings (Figures 3.3.1 - 3.3.4). There were higher frequency and intensity of rainfall for all duration lengths in the summer than in the winter. Spring and fall duration frequencies were greater than winter but less than summer. The annual and monthly trends were not as pronounced.

In an effort to further identify the nature of annual, monthly, and seasonal rain, the duration of selected rates were compared using an overlaid plotting structure. The seasonal results were plotted and displayed in Figures 3.3.1 through 3.3.4. Once again, the most differentiation was found between seasons. At this stage of the analysis, modifications were made to the plot routines. Options were added to the program parameters to define the length of the X-axis, convert abscissa and ordinate axes into logarithmic scale, or choose the form of the plots (e.g., black pen, red pen).

Onset and cessation of rainfall is variable. It may begin in one month or season and end in a subsequent one. This phenomenon can obscure the boundaries between January and February or Winter and Spring. To investigate this potential confound, the number of rainfall durations that crossed monthly or seasonal boundaries were examined. The frequency of crossovers were four in forty one seasons or approximately 10%.

WINTER PLOT FOR SIX DURATION TIMES

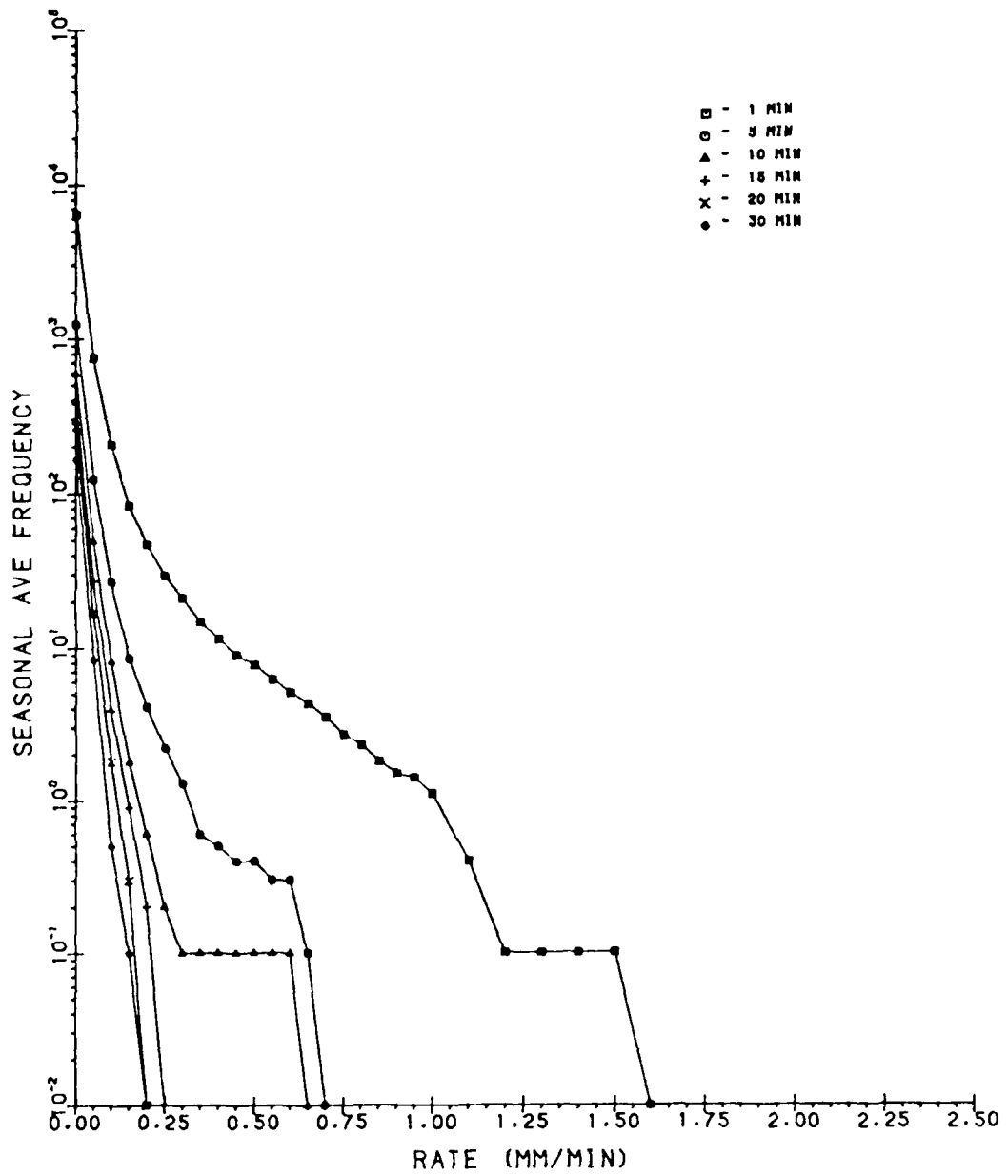


Figure 3.3.1

SPRING PLOT FOR SIX DURATION TIMES

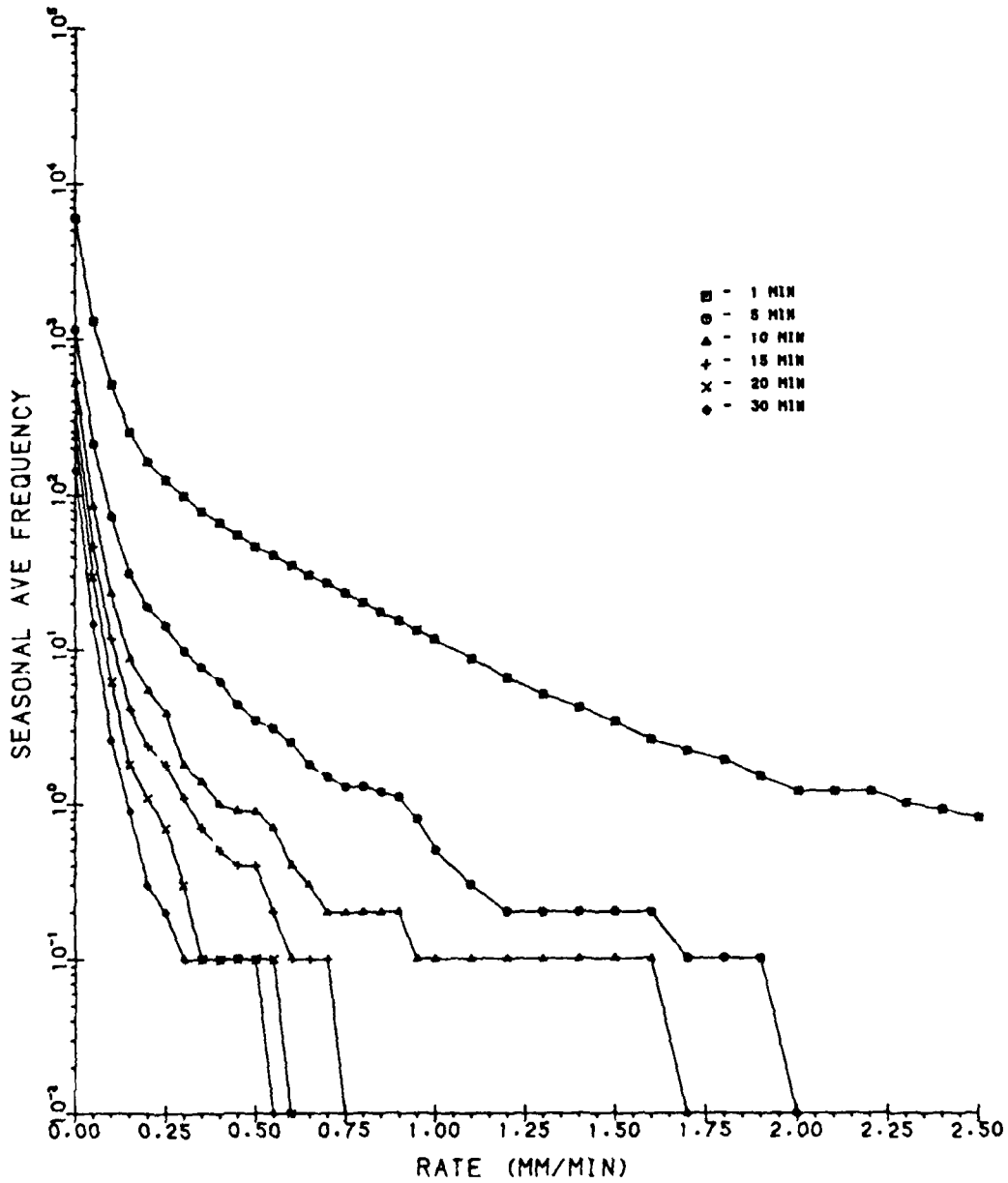


Figure 3.3.2

SUMMER PLOT FOR SIX DURATION TIMES

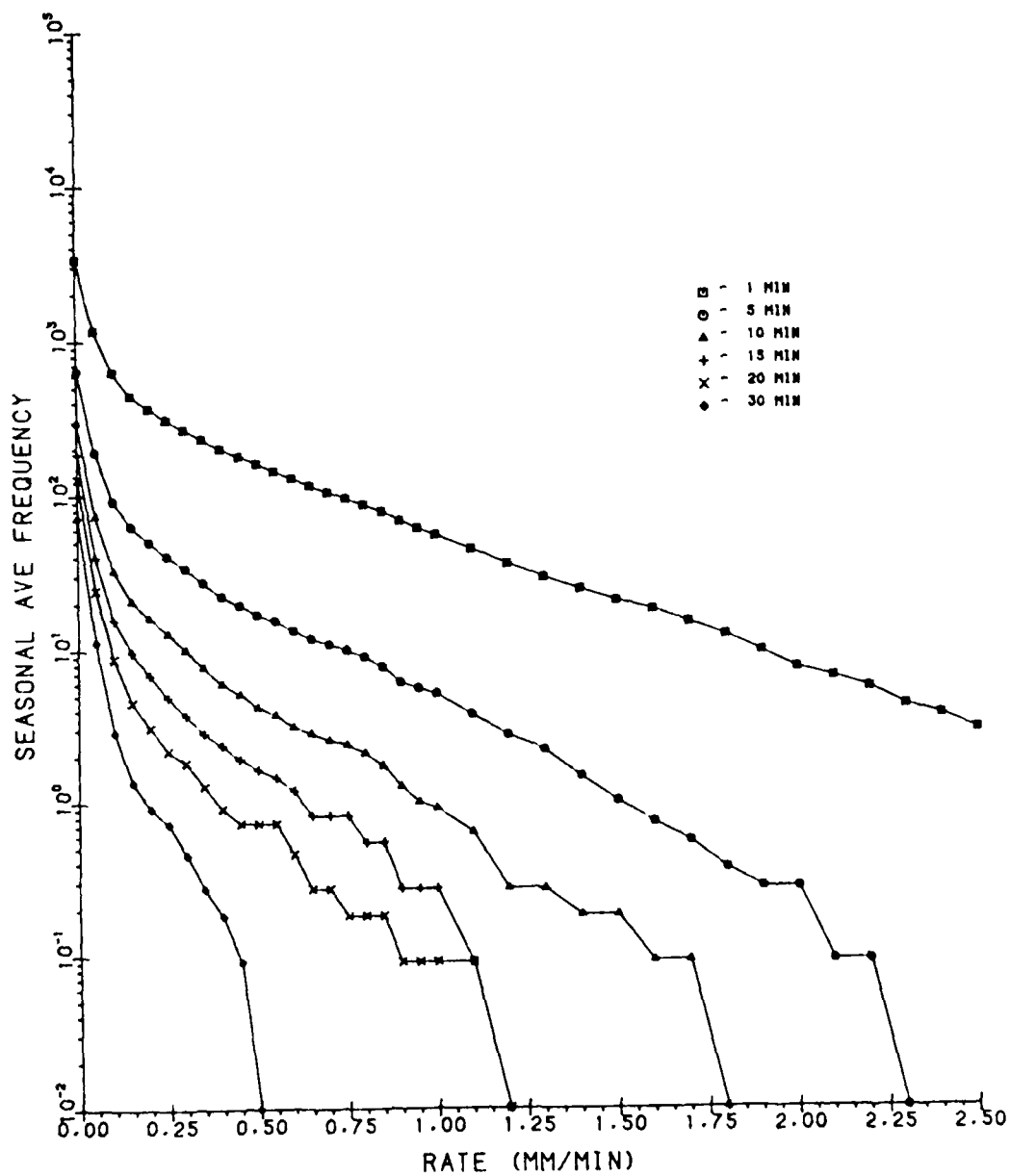


Figure 3.3.3

FALL PLOT FOR SIX DURATION TIMES

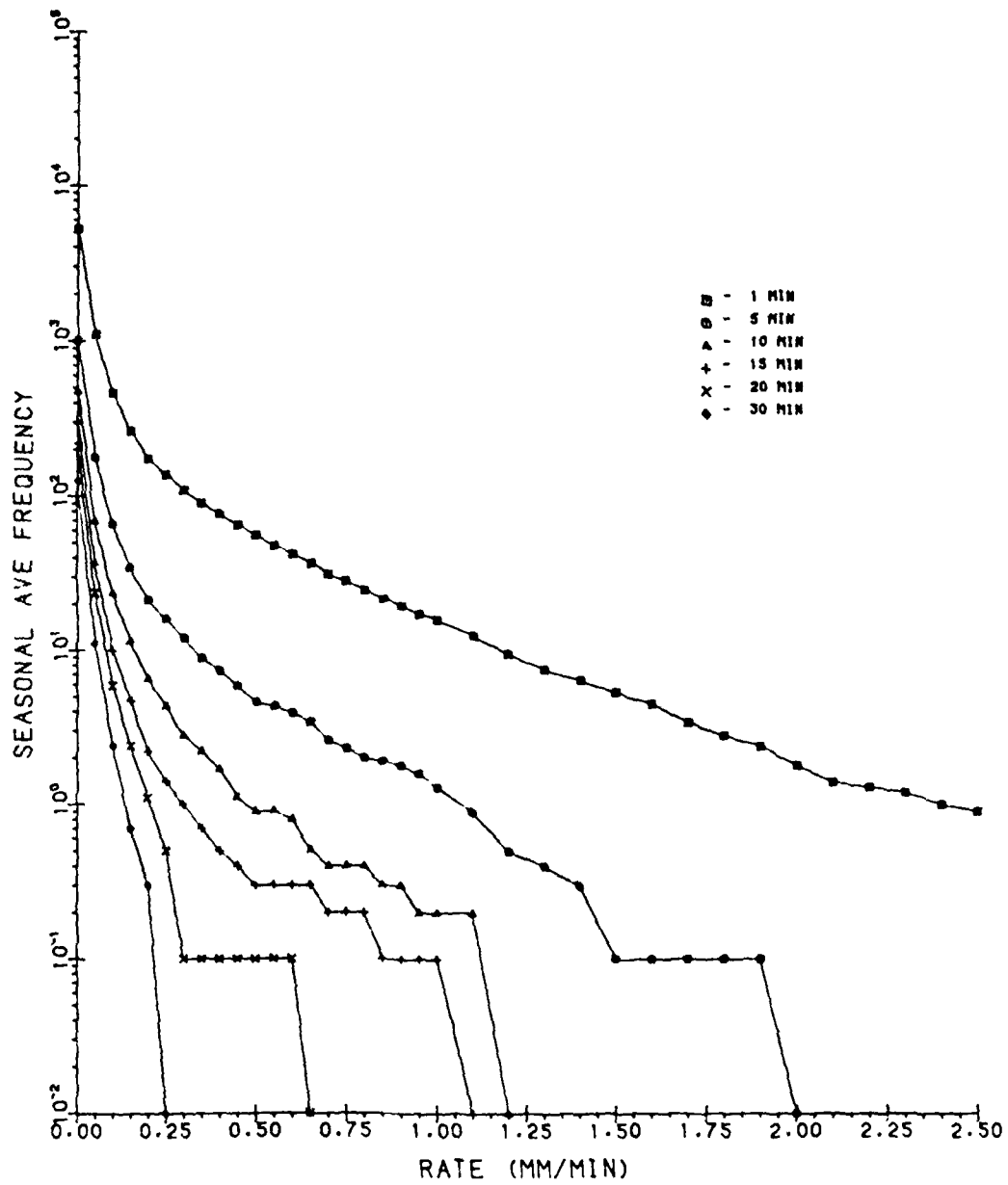


Figure 3.3.4

The crossovers were handled by placing the observation in the month or season where the majority of rainfall occurred.

The scope of the investigation was then directed toward the analysis of rainfall durations for monthly and seasonal categories. To determine more specifically if there was any clustering of long duration lengths by intensity levels, time frame (seasonal or monthly), or year; tables were constructed that listed the longest duration length the year that it occurred, and the threshold value that it exceeded. The seasonal table is presented in Appendix E. The data indicate that by season, the longest duration of rates greater than 0.1 mm/min is in the fall, followed by spring, summer and winter.

The next step was to find the probability of rainfall occurring at different intensities and durations. Since the frequency of rainfall was rare for intensities over 2.5 mm/min and durations greater than 30 minutes, a Poisson distribution was used. The probability of obtaining 1, 3, 5, 10, 10, or 20 occurrences of rainfall that exceeded intensities of .1 through 2.5 mm/min were plotted for 5, 10, 15, 20, and 30 minute durations and each season. Examples of some plots are displayed in Figures 3.3.5 and 3.3.6.

Although duration levels between 1 and 30 minutes were mostly examined in this study, continuous rainfall did reach limits of 1440 minutes. Using the intensity measures, which ranged between .001 and 10.5, it was possible to assess the relationship between rainfall intensities and durations for each season. There may indeed exist an asymptotic duration where rainfall is most intense. The findings of this analysis showed that no significant patterns were apparent.

The final breakdown of rainfall was done by time of the day. Two such analyses were conducted. The first presented rainfall intensities of .001, .25, .50, .75, 1.00, 1.50, and 2.0 mm/min for each individual hour from 0000 hours to 2400 hours. The second analysis aggregated these units into 6 4-hour intervals. Figures 3.3.7 - 3.3.9 exemplifies some seasonal hourly interval plots.

SUMMER PLOT - AT LEAST 1 OCC.

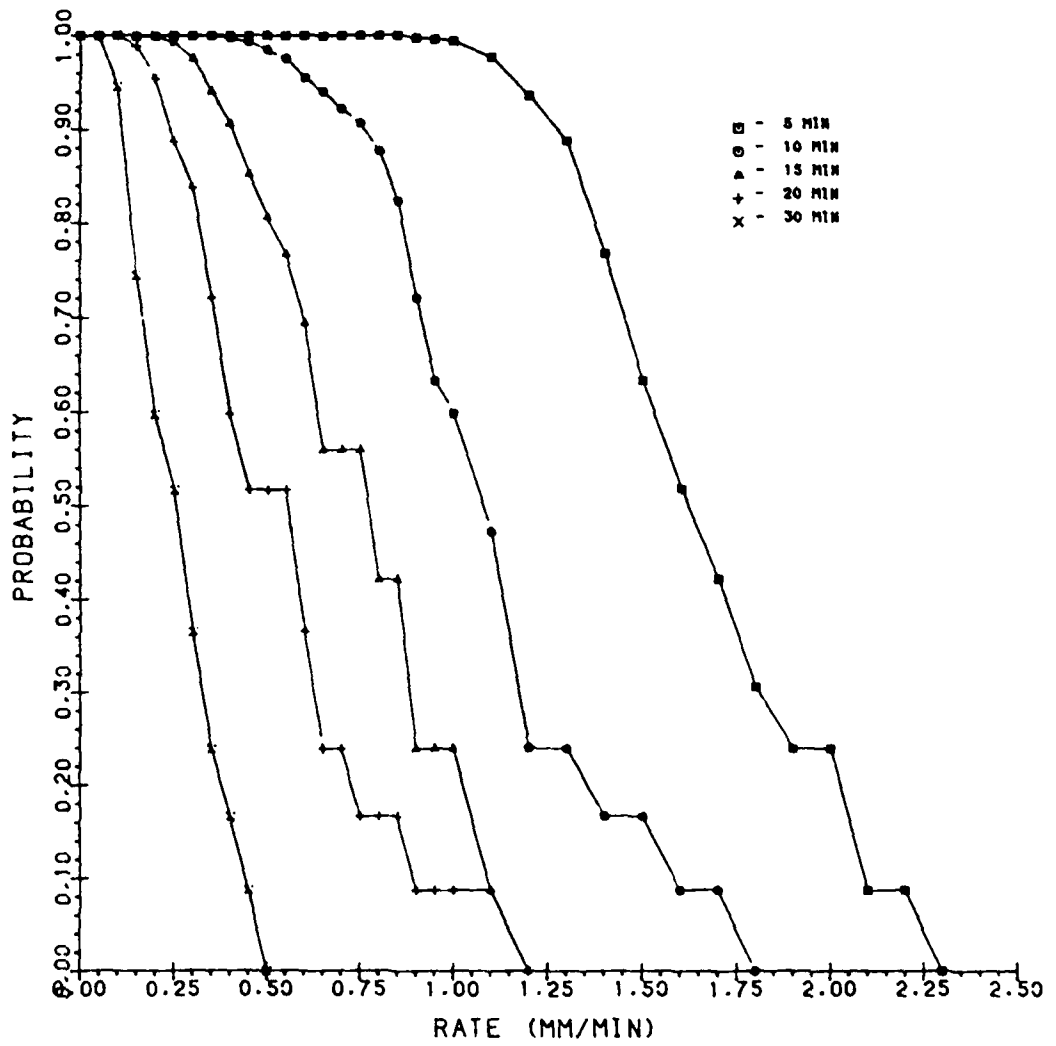


Figure 3.3.5

SUMMER PLOT - AT LEAST 5 OCC.

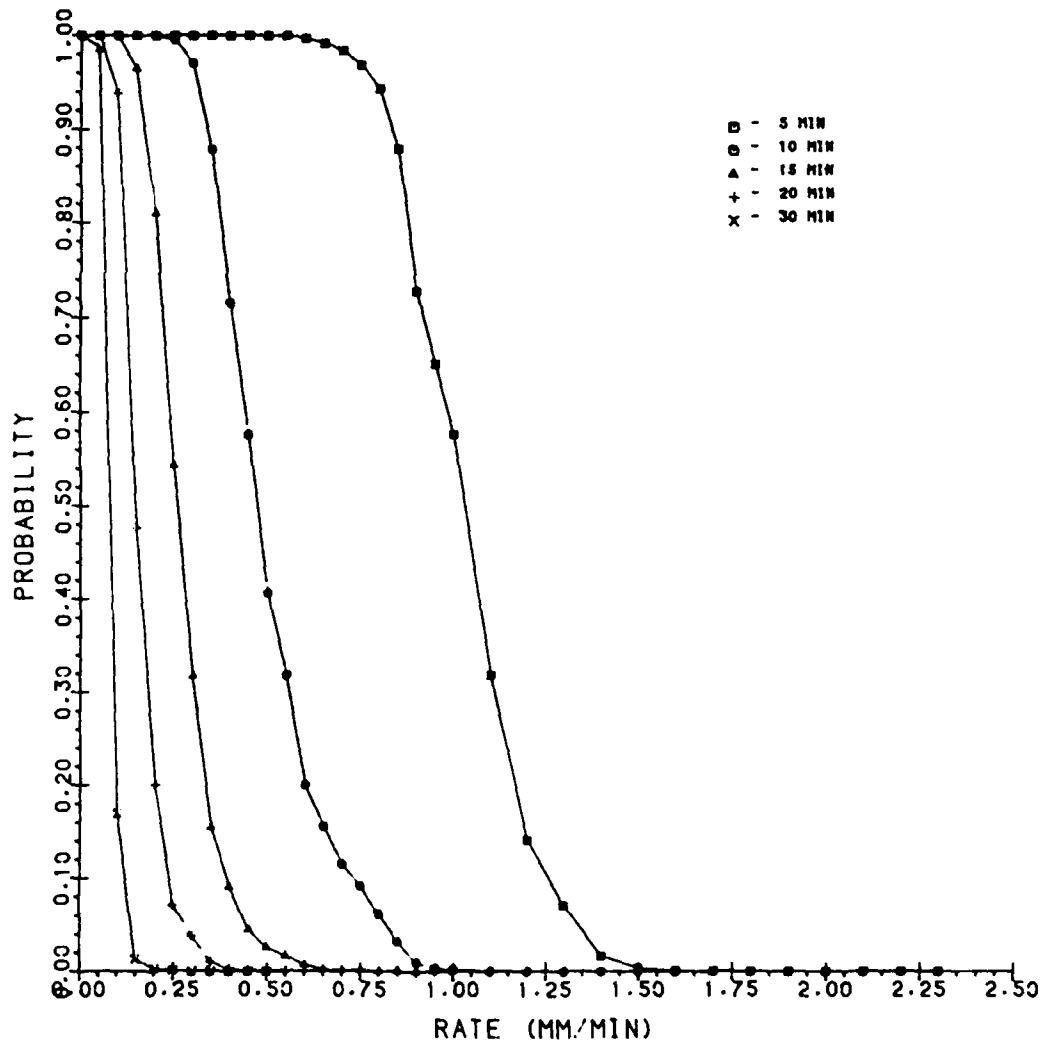


Figure 3.3.6

SUMMER : 0000-0400

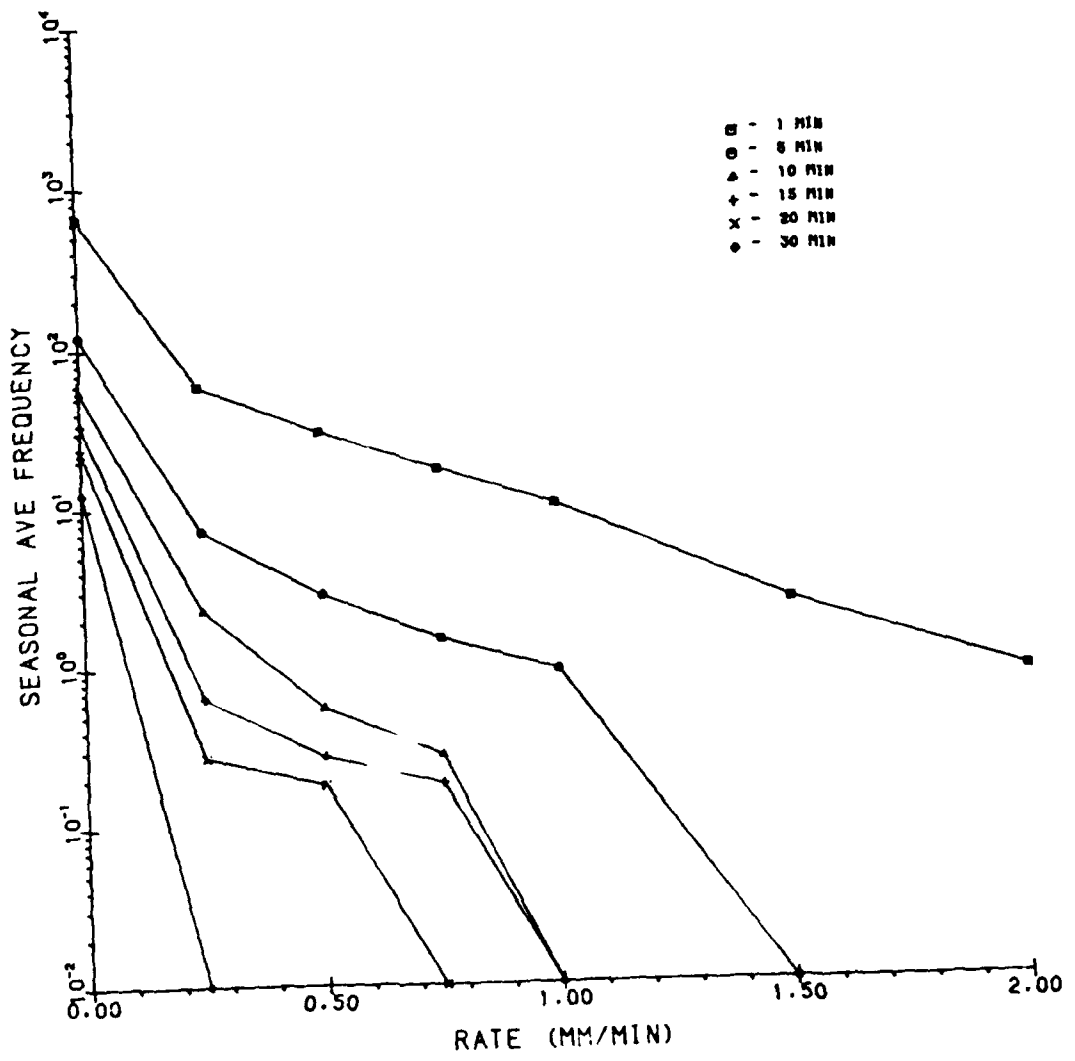


Figure 3.3.7

SUMMER : 1200-1600

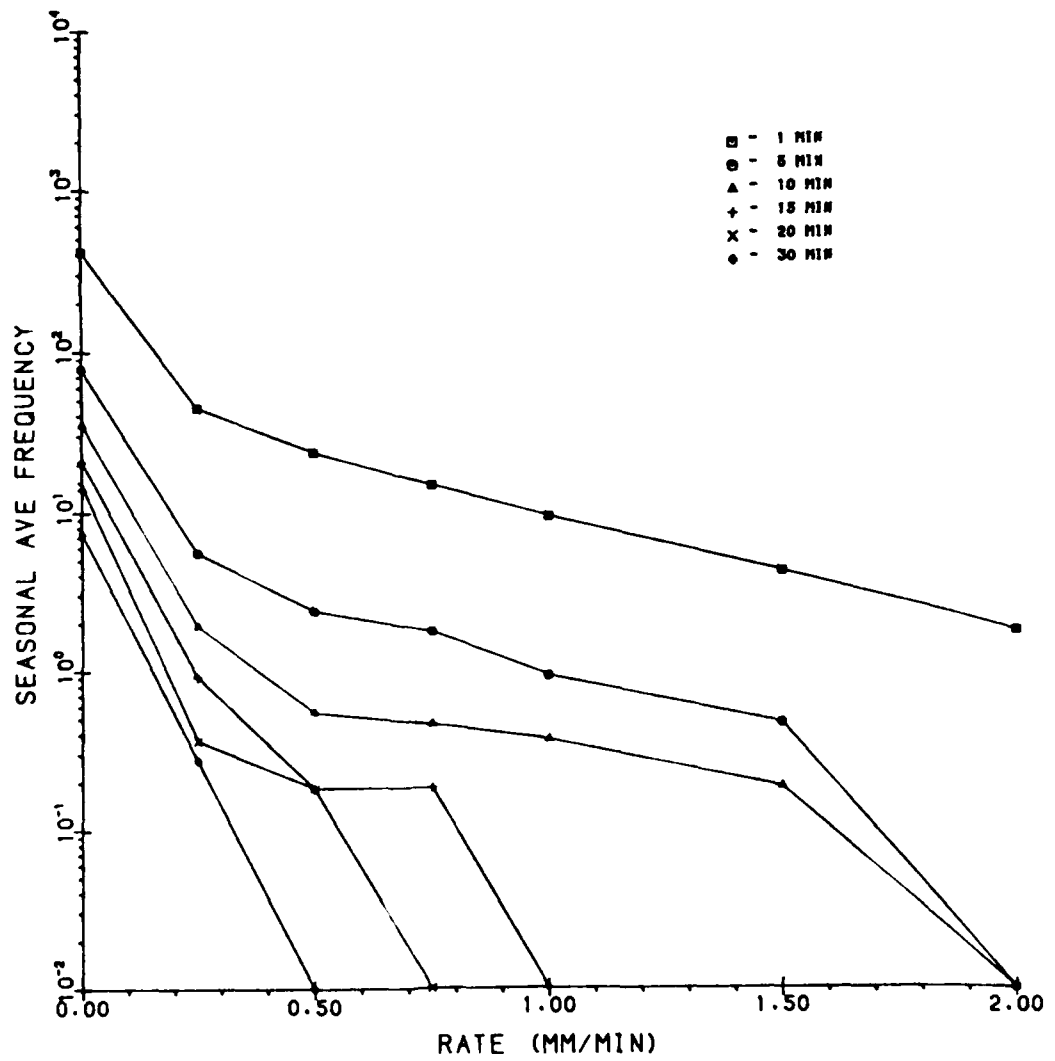


Figure 3.3.8

SUMMER : 2000-2400

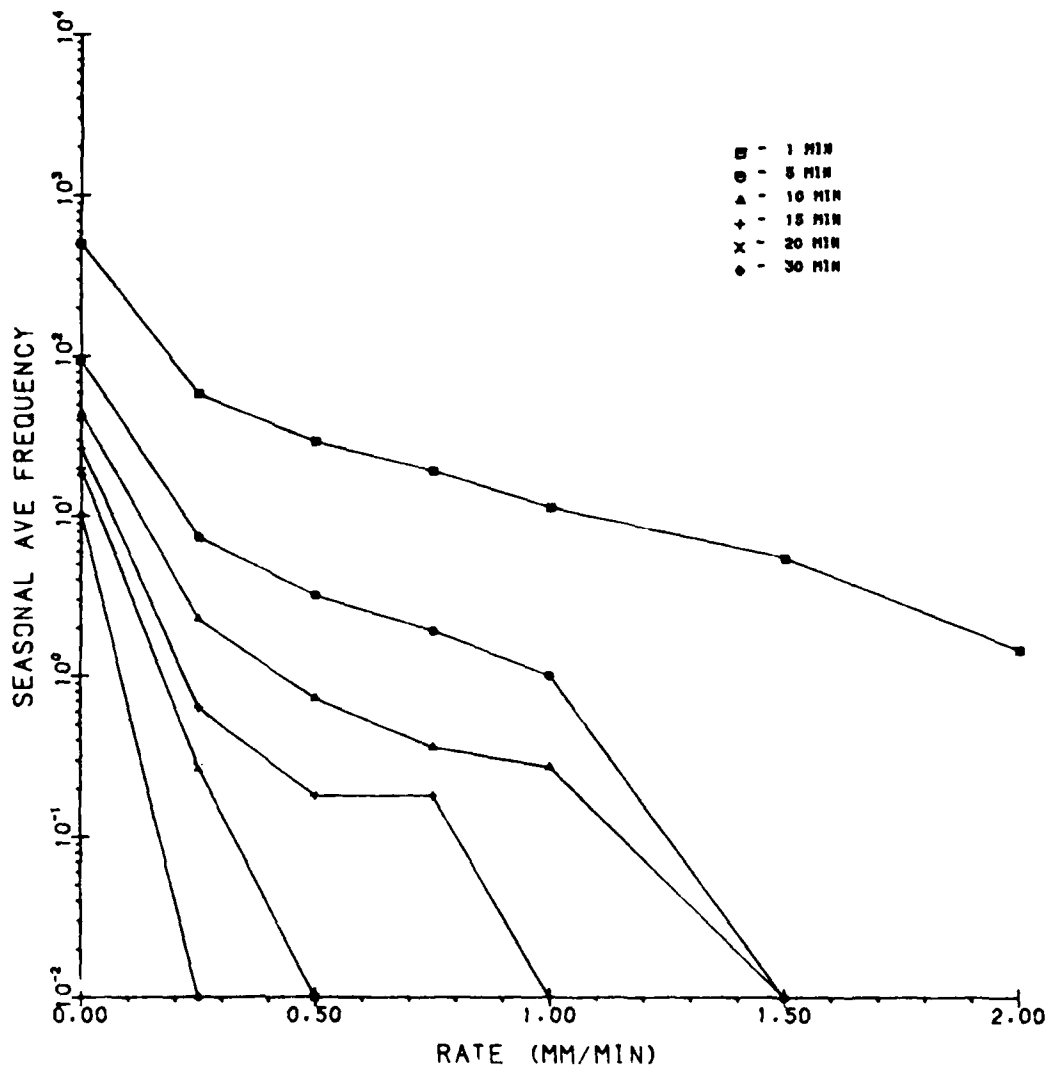


Figure 3.3.9

4.0 CONCLUSIONS

A model for estimating 1-minute rainfall rates has been developed using stepwise multiple regression analysis. It is made up of six regression equations to estimate rates that are equalled or exceeded 0.01, 0.05, 0.10, 0.50, 1.0, and 2.0 percent of the time during a month at a given location. The model is based on 122 months of data gathered from 12 stations (Tattelman and Scharr (1983)).

Tables and graphs presented in this paper were used as part of a presentation given at the 4th Conference on Applied Climatology, Scottsdale, Arizona, May 21- 24, 1984.

The Urbana data, extensively examined here, is the largest continuous, accurate and complete gathering of 1-minute instantaneous rainfall rates ever recorded. The analyses that have been done on this data base include detailed descriptive statistical information that will be used as a basis for comparison with other rainfall data sources. The software programs described in this report have been written with flexibility to allow data from other sources and other formats to be processed similarly.

Further effort is likely to include a modeling scheme where the estimate of frequency of occurrence of rain durations for varying rain intensities is done. The modeling equation will most likely be in non-linear exponential form.

REFERENCES

Tattelman, P., and Grantham D. D.: A Survey of Techniques for Determining Short-Duration Precipitation Rate Statistics. Air Force Surveys in Geophysics, No. 441, AFGL-TR-82-0357, ADA125705.

Tattelman, P., and Scharr, K. G.: A Model for Estimating 1-Min Rainfall Rates. Journal of Climate and Applied Meteorology, September, 1983.

APPENDIX A

Rainfall Tape Characteristics

Tape Name	KRAIN1	RAIN1
Label	Unlabeled	Unlabeled
Density (BPI)	800	1600
Record Length:		
Logical	253	80
Physical	253	800
Record Format	Fixed block	Fixed block
Track type	7	9
Character code	BCD	ASCII
No. of files	6	24

APPENDIX B

Tapel = RAIN1 (File 24)

File Description

<u>Column No.</u>	<u>Format</u>	<u>Variable Name</u>	<u>Identification</u>
1	F1.0	Code	0 = regular data record 1 = zero data record 2 = missing data record 3 = start record 4 = end record
2-3	F2.0	Station No.	Two digit station ID (Urbana, Ill = 11)
4-5	F2.0	Year	Year of recording 72 - 79
6-7	F2.0	Month	Month of recording 01 - 12
8-9	F2.0	Day	Day of recording 01 - 31
10-11	F2.0	Hour	Hour of recording 00 - 23
12-13	F2.0	Minute	Minute of recording 00, 15, 30 or 45
14-73	15F4.3	1-minute rates	15 1-min rates (mm/min) Rounded to nearest .001. Rates less than or equal to .0042 set to 0.0.

APPENDIX C

Tape2 = KRAIN1 (file 1)
File Description

<u>Column No.</u>	<u>Format</u>	<u>Variable Name</u>	<u>Identification</u>
1	F1.0	Code	0 = regular data record 1 = zero data record 2 = missing data record 3 = start record 4 = end record
2-3	F2.0	Station No.	Two digit station ID (Urbana, Ill = 11)
4-5	F2.0	Year	Year of recording 69 - 72
6-7	F2.0	Month	Month of recording 01 - 12
8-9	F2.0	Day	Day of recording 01 - 31
10-11	F2.0	Hour	Hour of recording 00 - 23
12-13	F2.0	Minute	Minute of hour 00
14-253	60F4.3	1-min rates	60 1-min rates (mm/min) rounded to nearest .001. Rates less than or equal to .0042 set to 0.

APPENDIX D

Frequency Distribution

<u>Bin Interval</u> (mm/min)	<u>Total Frequency</u> <u>in 10.25 years</u>
.001 - .05	169108
.05 - .10	24069
.10 - .15	7197
.15 - .20	2839
.20 - .25	1459
.25 - .30	1029
.30 - .35	841
.35 - .40	636
.40 - .45	470
.45 - .50	389
.50 - .55	345
.55 - .60	283
.60 - .65	236
.65 - .70	217
.70 - .75	178
.75 - .80	161
.80 - .85	147
.85 - .90	142
.90 - .95	113
.95 - 1.00	101
1.00 - 1.10	43
1.10 - 1.20	49
1.20 - 1.30	37
1.30 - 1.40	36
1.40 - 1.50	32
1.50 - 1.60	14
1.60 - 1.70	12
1.70 - 1.80	17
1.80 - 1.90	9
1.90 - 2.00	10
2.00 - 2.10	13
2.10 - 2.20	7
2.20 - 2.30	3
2.30 - 2.40	4
2.40 - 2.50	2
2.50 - 2.60	9
2.60 - 2.70	5
2.70 - 2.80	4
2.80 - 2.90	0
2.90 - 3.00	0
3.00 - 3.50	9
3.50 - 4.00	5
4.00 - 4.50	4
4.50 - 10.00	0

APPENDIX E

Longest Seasonal Duration Lengths

Threshold (mm/min)	Winter		Spring		Summer		Fall	
	length	year	length	year	length	year	length	year
0.1	48	1971	75	1976	69	1970	91	1969
0.2	18	1975	45	1976	36	1970	38	1969
0.3	13	1975	39	1976	33	1975	21	1978
0.4	12	1975	37	1976	32	1975	21	1978
0.5	12	1975	32	1976	26	1975	20	1978
0.6	10	1975	15	1974	26	1975	20	1978
0.7	4	1975	15	1974	25	1975	19	1978
0.8	3	1975	14	1974	23	1975	16	1978
0.9	2	1976	14	1974	22	1975	15	1977
1.0	2	1976	13	1974	20	1975	15	1977
1.3	1	1975	12	1974	14	1975	9	1977
1.6	-	-	10	1974	10	1977	6	1976
2.0	-	-	4	1974	5	1977	3	1976
2.5	-	-	4	1974	3	1972	2	1976

GRAVITY ANALYSIS

1.0 INTRODUCTION

1.1 Background

The Air Force Geophysics Laboratory (AFGL) is developing a program to verify gravity models by directly measuring gravity using high-altitude balloons. Gravity is measured using a very accurate vibrating string accelerometer (VSA) gravimeter as part of a balloon gondola package.

Although the gravimeter package senses the acceleration due to gravity, it also senses accelerations due to motion of the gondola package. These accelerations consist of translational accelerations of the gondola package as well as accelerations due to rotational motion of the gondola package, i.e., pendulum effects and rotations of the gondola package about its own axis.

The pendular motion of the gondola package also perturbs the gravity measurements in another way in that the deflection of the gondola package from the local vertical (the direction of the gravity vector) causes errors in the estimate of gravity at that point, since the gravimeter axis is no longer aligned with the local vertical.

Another important consideration in using this technique to estimate gravity is that accurate knowledge of the gravimeter's position is necessary to compare measured results with gravity models at the gravimeter location.

The long-term goal of this project is to determine gravity to 1 mgal accuracy. This "error budget" can be simply described in terms of the acceleration, velocity, and position of the gondola package and the deflection from the local vertical of the gondola package. Acceleration of the gondola package along the local vertical of 10^{-5} m/sec², or deflections of 0.08 degrees from the local vertical of the gondola package would cause gravimeter errors of 1 mgal. Also, a correction to the gravimeter measurement must be made that depends on the east-component of the gondola package's velocity. An error of 0.08 m/sec in the estimate of this velocity would cause an error in the gravity estimate of 1 mgal. Also,

since gravity varies in the vertical direction roughly as 1 mgal per 3 meters, errors in the estimate of the gondola package of 3 meters would also cause gravity estimate error of 1 mgal.

Given that the actual acceleration, deflection, horizontal velocity and position errors are orders of magnitude larger than the limits shown, using unprocessed gravimeter data as the gravity estimate would be completely unsatisfactory. The solution proposed by AFGL involves the accurate determination of the motion of the gondola package (position, velocity, acceleration, and rotation) and use of this information to correct the gravimeter's measurement. The combination of an accurate tracking system and an inertial motion sensing package (IMSP) is required in order to estimate gondola position, velocity, and acceleration accurately.

In October 1983, a launch of a high-altitude balloon was conducted by AFGL personnel at Holloman AFB in New Mexico. The balloon gondola package included a VSA gravimeter and an inertial motion sensing package which included 3 orthogonal accelerometers, 3 orthogonal rate gyros, and 3 orthogonal magnetometers. Gondola position tracking was done by three ground-based digital radars located at White Sands Missile Range (WSMR).

The objectives of this flight were to demonstrate the feasibility of measuring gravity using a high-altitude balloon and to evaluate the performance of the digital radar in tracking the balloon. The objective of this flight was not to estimate gravity to 1 mgal accuracy, although it was hoped that the data could be processed in some way to improve the raw gravimeter output.

1.2 Overview

BEDFORD RESEARCH's participation in the post-flight data analysis included the creation of an investigator's data tape and the support of AFGL personnel in their analysis of gravimeter, tracking, and IMSP data. The investigator's data tape is a data base consisting of evenly-sampled data from the VSA gravimeter, IMSP, digital radar, and other sources.

The following 3 sections of this report will describe 3 separate technical projects involving the processing of the balloon gravity data. Section 2.0 describes an algorithm used to predict missing data found in the radar tracking channels. Section 3.0 describes a computer program which allows users to read selected time segments and channels of the investigator's data tape interactively and to place these data into separate I*S*P data files for subsequent processing and analysis. Finally, Section 4.0, describes some analysis of the radar tracking data which was intended to get a better estimate of the balloon trajectory. This analysis involved the use of a Kalman filter to incorporate radar tracking data and VSA data in order to smooth the vertical position estimate of the gondola location.

2.0 PREDICTION FILTER TO FILL IN GAPS OF RADAR TRACKING DATA

2.1 Introduction

One of the problems encountered during the post-flight data analysis was the existence of numerous data gaps in the WSMR radar tracking data. The presence of gaps in the data can cause severe problems for tracking algorithms, and may have caused problems for DMA in deriving gravity estimate values from tracking data. For these reasons an algorithm was developed to predict the missing data to preserve its continuity.

Sixty-one gaps were identified which ranged from 2 to 30 samples in length. In addition, three large gaps were identified which were 259, 199, and 839 samples long. Because of their length, these gaps were not filled since the performance of any algorithm would be highly suspect over such long periods.

This section presents the algorithm used to predict the missing data. This algorithm is based on the theory of linear prediction [1]. Following a discussion of the algorithm, a brief discussion of its implementation and some graphical results are presented.

2.2 Linear Prediction Algorithm

The approach taken to fill in the gaps is to use the technique of linear prediction. This technique assumes an auto-regressive (AR) time series model for the data, and uses this model to predict the missing data based on the existing data surrounding the gap. The signal $x(n)$ is assumed to be a linear combination of past values and some input $u(n)$:

$$x(n) = \sum_{k=1}^P a_k x(n-k) + u(n) \quad (1)$$

The input $u(n)$ is assumed to be a white noise term with variance σ^2 . The model order P must be estimated and the AR coefficients $\{a_k\}$ must be determined. Experiments with the tracking data showed that $P=8$ is a good model order to use.

The sample values $x(n_0), x(n_0+1), \dots, x(n_1)$ are assumed to be missing. Thus, the gap is $L=n_1-n_0+1$ points wide.

The data immediately preceding the gap are used to estimate the forward prediction coefficients $\{a_k\}$ via the Burg method [2]. This method is part of the basic I*S*P package under the function name LNP. 500 points are used to form the estimates. These prediction coefficients are used in the following formula to yield the forward prediction data:

$$\hat{x}_f(n) = \sum_{k=1}^P a_k \hat{x}_f(n-k), \quad n=n_0, n_0+1, \dots, n_1 \quad (2)$$

where $\hat{x}_f(n)=x(n)$ for $n < n_0$.

Similarly, the data immediately following the gap are used to estimate the backward prediction coefficients $\{b_k\}$. Again, the Burg method is used and 500 points are used to form the estimate. The backward prediction coefficients are used in the following formula to form the backward prediction data:

$$\hat{x}_b(n) = \sum_{k=1}^P \hat{b}_k x_b(n+k), \quad n=n_1, n_1-1, \dots, n_0 \quad (3)$$

where $x_b(n)=x(n)$ for $n>n_1$.

The final prediction estimate $x(n)$ is formed by adding a weighted version of the forward and backward estimates. The weights are proportional to the error in the predictors where the error will increase as n is farther away from n_0 for the forward predictor and n_1 for the backward predictor. The final prediction equation is then given by:

$$\hat{x}(n_{0+m}) = \left(\frac{L-1-m}{L-1} \right) \hat{x}_f(n_{0+m}) + \left(\frac{m}{L-1} \right) \hat{x}_b(n_{0+m}), \quad (4)$$

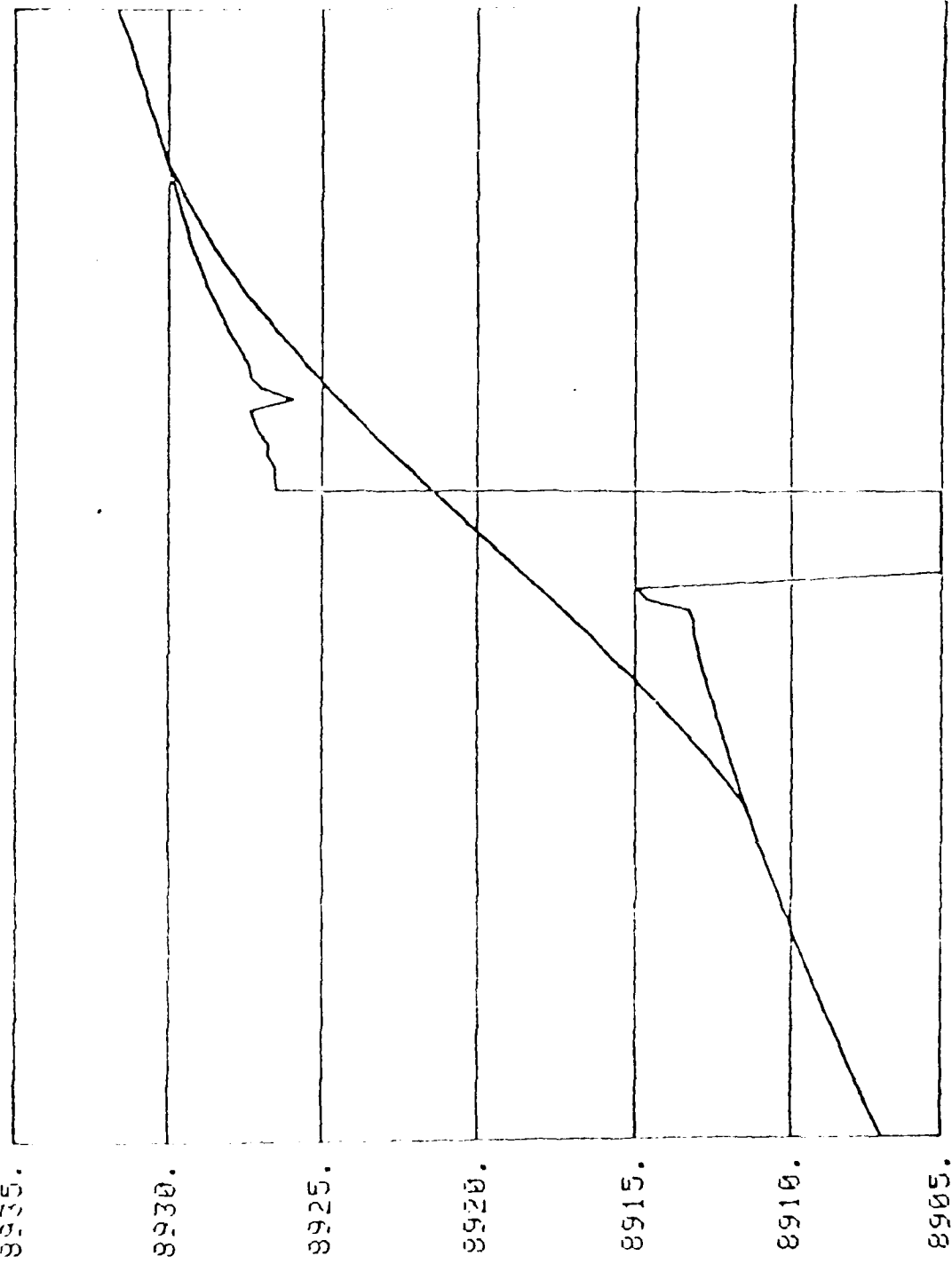
$$m = 0, 1, \dots, L-1$$

2.3 Implementation Issues

If the data have a DC offset and/or linear trend, they can cause errors in estimating the prediction coefficients and will adversely affect the prediction results. Therefore, the DC offset and trend are first removed from the data preceding the gap and from the data following the gap before estimating the prediction coefficients. The forward and backward prediction coefficients are then computed from the detrended data. The detrended forward and backward predictions are then computed using (2) and (3). The DC offset and trend are then added back to the predictions and the weighting in (4) is finally applied.

One problem that was encountered during the graphical inspection of the gaps was that, very often, the data immediately surrounding the gaps seemed to be suspect. This is shown in Figs. 2.1-2.3 where the gap is indicated by the two vertical lines. Note that Figs. 2.2 and 2.3 show two gaps in the time span shown. These figures show that the data just before the gap and just after the gap are noisier than data further away from the gap. For this reason it was decided to extend the size of the gap (or to predict more points) for gaps that showed this tendency. Also displayed in Figs. 2.1-2.3 are the predictions for these gaps. These are the smooth curves that pass over the gaps. In Figs. 2.2 and 2.3 where two gaps are so closely located, the two gaps are treated as a single gap.

SEGMENT 1 RECORD 26

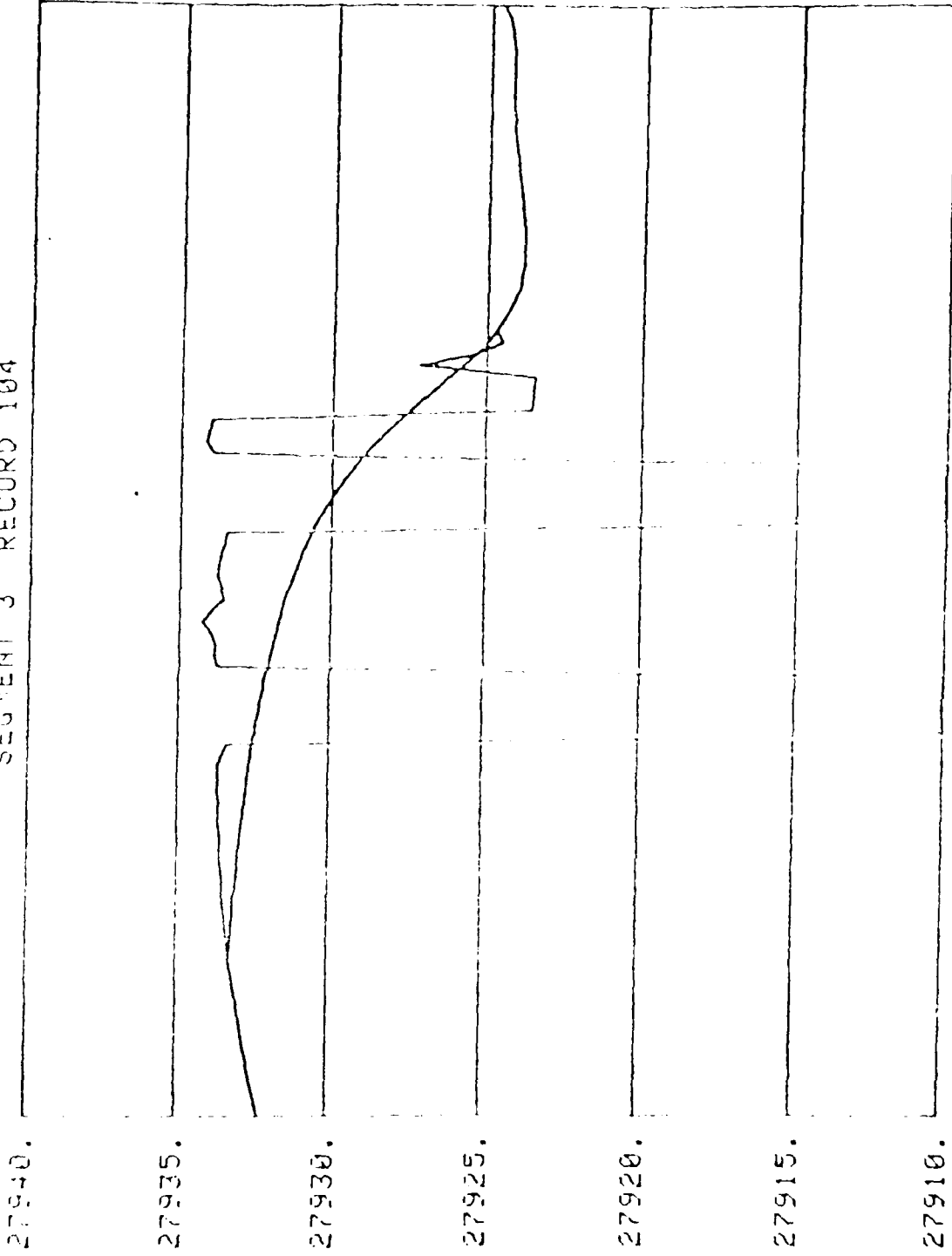


ISP>

TIME

Figure 2.1 - Example of a gap of 8 points in WSMR tracking data. Gap is indicated by the 2 vertical lines in the plot. Also shown is the predicted data which is the smooth line through the gap. Note that the predicted data actually spans more points than the gap alone due to the larger fluctuations in the data surrounding the gap.

SEGMENT 3 RECORD 104



ISP

TIME

Figure2.2 - Example of section of data with two gaps, each of length 6. Each gap is indicated by 2 vertical lines in the plot. Also shown is the predicted data which is the smooth line through the gaps. Note that the predicted data actually spans more points than the gaps alone due to the larger fluctuations in the data surrounding the gaps.

SEGMENT 3 RECORD 173

26725.

26720.

26715.

26710.

26705.

26700.

26695.

64190.

:SP>

TIME

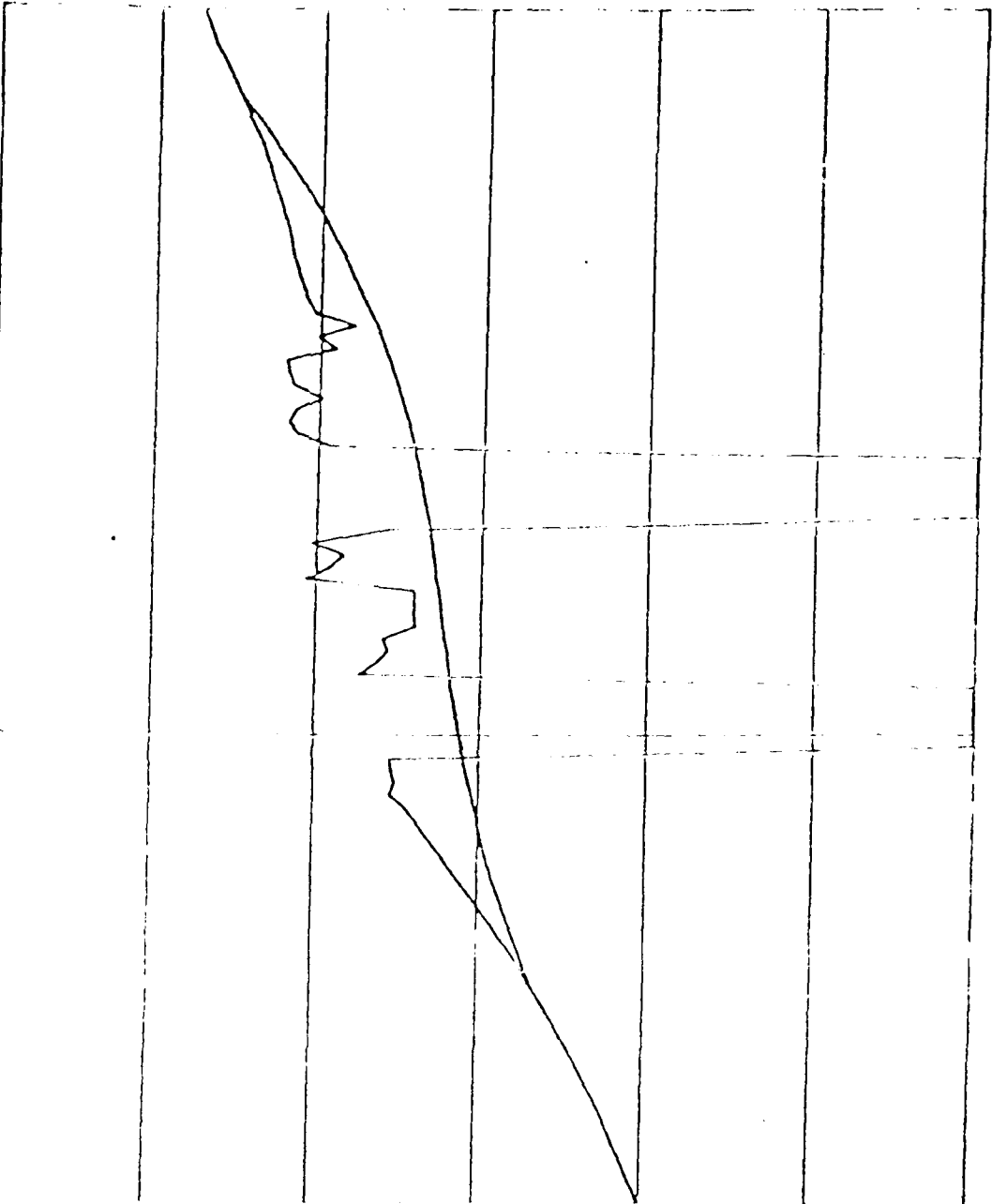


Figure 2.3 - Example of section of data with two gaps, each of length 6. Each gap is indicated by 2 vertical lines in the plot. Also shown is the predicted data which is the smooth line through the gaps. Note that the predicted data actually spans more points than the gaps alone due to the larger fluctuations in the data surrounding the gaps.

3.0 PROGRAM TO READ INVESTIGATORS' DATA TAPE

3.1 Introduction

The investigators' data tape (IDT) is a unified data base containing 48 channels of data plus time code. The data were put on the tape at a sample rate of 10 Hz.

This section briefly describes a FORTRAN program written to allow users to interactively read selected time segments and channels of this file and place the data into separate I*S*P data files for subsequent processing and analysis.

3.2 Program Description

A FORTRAN program was written to allow users to interactively access the IDT and place particular channels and time segments into I*S*P files for further analysis.

The program will prompt the user for the necessary input and output information and then open the IDT (which is actually a disk file on the VAX), read the appropriate channels, and write the specified I*S*P files.

The program begins with the following prompts:

Enter start time (Zulu) below :

Enter hours :

Enter minutes :

Enter seconds :

The user should type in the time at which to begin reading the IDT as integers by first specifying the time in hours, then minutes, then seconds.

The user will then be prompted for the amount of time he wishes to read in the same way he was prompted for the start time:

Enter amount of time to read below:

Enter hours :

Enter minutes :

Enter seconds :

Next, the following prompt appears:

Enter decimation/averaging factor :

The user should enter 1 if he wishes to preserve the original 10 Hz sampling rate, or an integer greater than 1 if he wishes to decimate or average the data. Caution should be taken when choosing a factor greater than 1 since aliasing will occur. The proper way to perform sampling rate decimation is to choose a decimation factor of 1 and then use the I*S*P program SRC to decimate or interpolate the files to the desired output sampling rate using the proper decimation/interpolation techniques [3].

If a decimation factor other than 1 is chosen, the following prompt appears:

Enter A for average or D for decimation :

If A is selected, n samples will be averaged to form an output value and the output samples will be separated by $0.1n$ sec, where n is the decimation/averaging factor. If D is selected, every nth sample will be output and again, the output samples will be separated by $0.1n$ sec.

The program will then inform the user how many records will be written, the record size, the amount of time to be read, and will ask if that is acceptable by typing the following prompt:

Is that OK (Y or N)? :

The user should respond with a Y for yes or an N for no. If Y is typed, the program will proceed and if N is typed, the program will go back to the beginning and prompt for the starting time at which point the user can type in new values.

The next prompt is:

Enter number of channels to write :

The user can then respond with an integer from 1-48.

The next prompt is:

Enter channel number (0 for menu) :

The program will type this prompt from 1 to 47 times, depending on the number of channels entered in the previous prompt. If 48 is entered, all channels will be written so the user is not prompted for channel numbers. If a 0 is typed, a menu of the 48 channels is typed on the screen.

The last prompt is:

Enter first ISP file number for output :

The user should enter an integer from 0-999. In the current version, if more than one channel is written, an I*S*P file is written for each channel and the numbering is consecutive starting at the number typed in for the first file. In future versions this may be changed to take advantage of I*S*P's multichannel file capability.

The following is a sample output from the program.

Enter start time (Zulu) below :

Enter hours : 17

Enter minutes : 52

Enter seconds : 0

Enter amount of time to read below:

```
Enter hours   : 0
Enter minutes : 10
Enter seconds : 0
Enter decimation/averaging factor : 1
Records to be written: 3
Record size: 2048
Amount of time to be read: 0 hr 10 min 14 sec
Is that OK (Y or N)? : Y
Enter number of channels to write : 2
Enter channel number (0 for menu) : 29
Enter channel number (0 for menu) : 38
Enter first ISP file number for output : 900
    1
    2
    3
Number of records written=      3
FORTRAN STOP
```

4.0 KALMAN FILTER TO SMOOTH TRACKING ESTIMATES

4.1 Introduction

Inspection of WSMR tracking data and errors raised some questions as to the validity of the error estimates. WSMR reported tracking errors on the order of 3 m for much of the flight, but visual inspection of these data along with an understanding of the basic physics of the balloon gondola package imply that the dynamics seen in the data are unreasonable and unrealistic. It was therefore postulated that the errors as reported by WSMR are overly optimistic.

To try to get a better estimate of the balloon trajectory, a Kalman filter was designed to incorporate both tracking data and accelerometer data from the gondola package. Section 4.2 is devoted to a description of the model and assumptions used to yield the estimate of the balloon trajectory, and Section 4.3 shows the results of the Kalman filter output.

4.2 Kalman Filter Design

For simplicity only the vertical direction was considered. The radar tracking data had been converted to geodetic coordinates so the geodetic height as determined by WSMR radar was used for the analysis. It was also assumed that, at float, the balloon pendulous motion was small so that the z-accelerometer and VSA were reasonably aligned with the local vertical, or geodetic height direction. The gondola geodetic height, h , velocity, dh/dt , and acceleration, d^2h/dt^2 are modelled in a three state Kalman filter model as:

$$x(k+1) = x(k) + Gu(k)$$

$$x(k+1) = \begin{bmatrix} 1 & \Delta & .5\Delta^2 \\ 0 & 1 & \Delta \\ 0 & 0 & \alpha \end{bmatrix} x(k) + \begin{pmatrix} 0 \\ 0 \\ 1 \end{pmatrix} u(k)$$

where $x(k) = (x_1(k) \ x_2(k) \ x_3(k))^T$, $x_1(k) = h$, $x_2(k) = dh/dt$, $x_3(k) = d^2h/dt^2$, and $\Delta = 0.1$ sec is the sampling interval. For the data segment used (a ten minute period starting at 1752 Zulu), the following parameters are valid:

$$\alpha = 0.994$$

$$q = E[u^2(k)] = 1.42 \times 10^{-8}.$$

The observations used are the geodetic height as determined by WSMR and the VSA output. The geodetic height was first pre-processed by subtracting the value of the first point so that the observations would start at zero. The VSA data was pre-processed by removing the mean value (due mainly to gravity), and by converting to units of m/sec^2 .

In the Kalman filter formalism the observations are written as

$$z(k) = \begin{pmatrix} h(k) \\ \frac{dh(k)}{dt} \end{pmatrix} + \begin{pmatrix} v_1(k) \\ v_2(k) \end{pmatrix}$$

$$z(k) = \begin{bmatrix} 1 & 0 & 0 \\ 0 & 0 & 1 \end{bmatrix} x(k) + v(k)$$

where $z(k)$ and $v(k)$ are (2 X 1) dimension vectors representing the observation vector and the observation noise vector respectively. The observation noise has a covariance matrix defined by

$$R = E[v(k)v(k)^T]$$

$$= \begin{bmatrix} 100 & 0 \\ 0 & 2.5E-7 \end{bmatrix}$$

Note that the values used here imply a standard deviation of 10 m for the tracking data and $5E-4$ m/sec² for the VSA data. The 10 m standard deviation for the tracking data is roughly 10 times larger than the values given by WSMR.

4.3 Results

Using the model developed and the parameters shown in Section 4.2, the Kalman filter was implemented to obtain estimates of the state vector $x(k)$ for the time period shown in Fig. 4.1. The result for the geodetic height $h=x_1(k)$ is shown in Fig. 4.2. The ragged curve is the original observations as seen in the top curve in Fig. 4.1 and the smooth curve is the Kalman filter output estimate for the geodetic height $h=x_1(k)$.

These results offer more evidence that the errors given by WSMR are overly optimistic. Noting the excursions in the original observations, it is clear that the errors are much greater than the 3 m reported by WSMR.

AD-A169 277

MATHEMATICAL AND STATISTICAL ANALYSIS(U) BEDFORD
RESEARCH ASSOCIATES MA F BATTLES ET AL. OCT 85
AFGL-TR-85-0336 F19620-02-C-0139

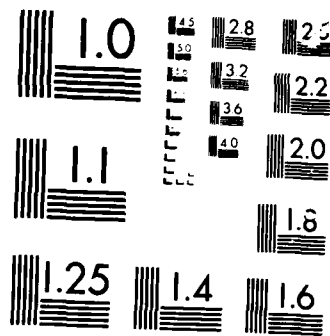
2/2

UNCLASSIFIED

F/G 4/1

NL





MICROCOPY

31731

6144.

本

100.

200.

300.

400.

500.

600.

700.

800.

-20.

-40.

0.006

0.004

0.002

0.

-0.002

-0.004

-0.006

-0.008

0. 100. 200. 300. 400. 500. 600.

TIME

Figure 41 - Observations used as inputs to the Kalman filter. Top curve is the geodetic height in meters with the initial value subtracted off. Initial value is 30218.2 m. Second curve is VSA data in units of m/sec² with the mean value subtracted. Time units are seconds with a start time of 1752 Zulu.

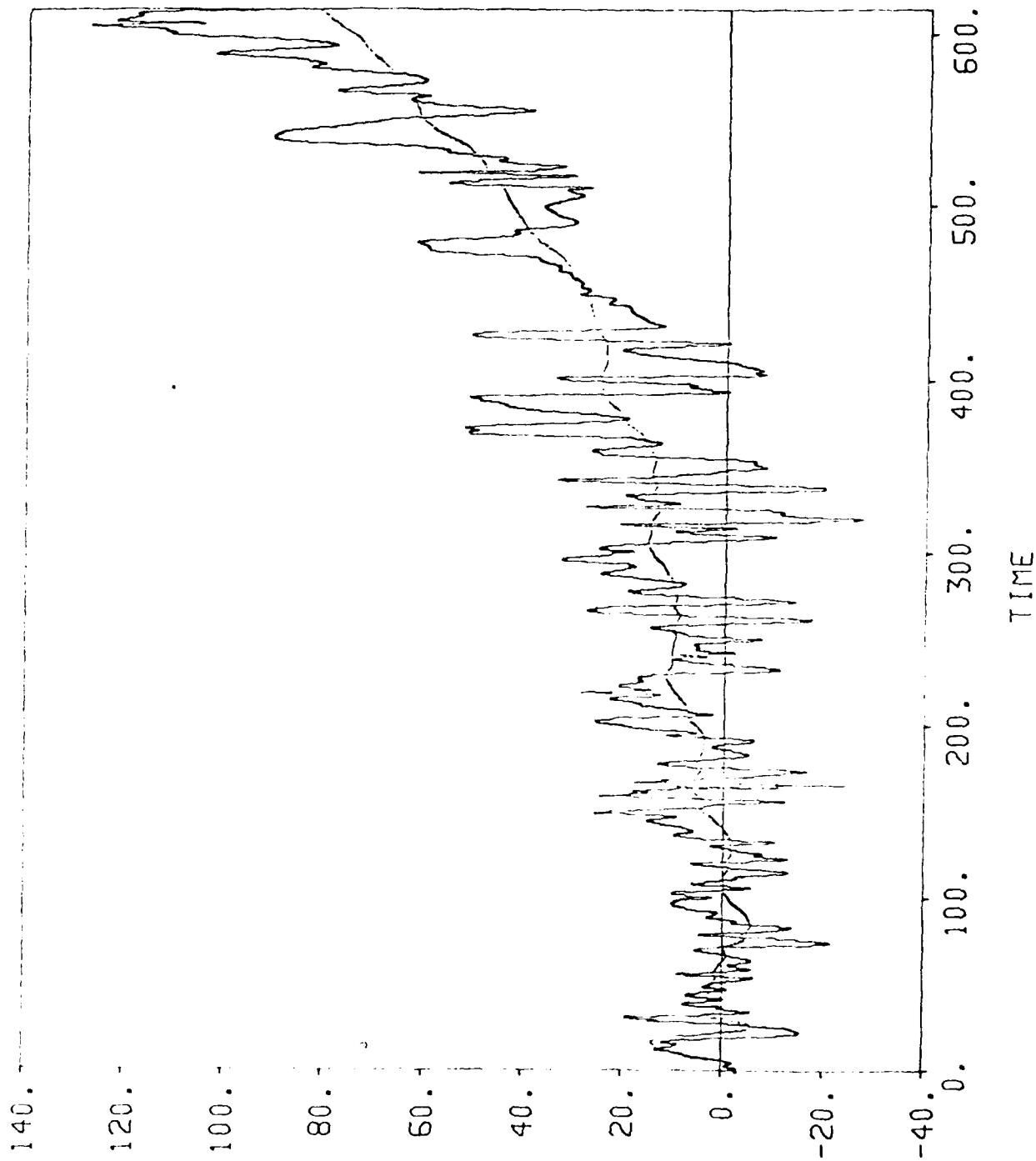


Figure 4.2 - Kalman filter estimate of geodetic height. Ragged curve are observations seen in top trace in Fig. 1. Smooth curve is the output of the Kalman filter.

REFERENCES

1. Makhoul, John, "Linear Prediction: A Tutorial Review," Proc. IEEE, Vol. 63, No. 4, April 1975.
2. Burg, John P., Maximum Entropy Spectral Analysis, Stanford University Ph.D. Thesis, 1975.
3. Crochiere, R.E., and Rabiner, L.R., "Interpolation and Decimation of Digital Signals - A Tutorial Review," Proc. of IEEE, Vol. 69, No. 3, March 1981.

THEORY AND MODELING OF INFRARED EMISSION

1.0 INTRODUCTION

The work consists of generating and maintaining computer codes and other software involved in the generation of predictive codes of infrared emission from quiescent and disturbed atmospheres.

2.0 DATA ANALYSIS

2.1 Data Modeling

The first project undertaken was the generation of code to fit a synthetic spectrum to the nitric oxide (NO) molecular fundamental vibration-rotation bands near $5.3 \mu\text{m}$ wavelength (1890 cm^{-1} frequency) by using nonlinear minimization techniques. The parameters to be fit were the number densities of molecules in the upper vibrational state (v') of the transition, that is, $n_{v'}$ (molecules/ cm^3) and temperature (T). The fitting problem is nonlinear in temperature T , but linear in the vibrational populations $n_{v'}$.

The quantity to be minimized (Φ) was the mean-square error between the measured spectral radiance $I_{\text{exp}}(\nu)$ (photons/ $\text{cm}^2 \text{sec sr cm}^{-1}$) (sr = star radians) where ν is the frequency in wavenumber (cm^{-1}), and the calculated synthetic spectral radiance $I(\nu, \{n_{v'}\}, T)$. Φ is given by

$$\Phi(n_{v'}, T) = \int_{\nu \text{ min}}^{\nu \text{ max}} d\nu [I(\nu, \{n_{v'}\}, T) - I_{\text{exp}}(\nu)]^2$$

The spectrum is sampled at 0.25 cm^{-1} intervals.

The form of the synthetic spectrum I is as follows:

$$I_{ul} = \frac{A_{ul} \Delta S}{4} n_{v'} g_j' \frac{e^{[-c_2(E' - E_{v'} / 21) / T]}}{Q_v(T)}$$

where

A = the Einstein A- coefficient in (sec^{-1})

$n_{v'}$ = the population density (molecules/ cm^3)

$g_{j'}$ = degeneracy of the state $j' = 2j' + 1$

c_2 = second radiation constant = 1.4388 k/cm^{-1}

E' = energy of the upper level

$E_{v',1/2,1}$ = the energy of state when $= v', j = 1/2, i = 1$

Δs = an effective path length

ul means: from the upper transition ($v'j'i'$) to the lower transition
($v''j''i''$)

$Q_{v'}(T)$ = partition sum

$$= Q_{v'}^{(\text{rot})}(T) \cdot Q^{(\Omega)}(T)$$

$$Q_{v'}^{(\Omega)}(T) = 1 + e^{-c_2 \Delta / T}$$

$$\Delta = E_2 - E_1 = 120 \text{ cm}^{-1}$$

$$Q_{v'}^{(\text{rot})}(T) = \frac{T}{c_2 B_{v'}} e^{[3c_2 B_{v'} / 4T]}$$

$$B_{v'} = 1.6 - 1.7 \text{ cm}^{-1}$$

To about 1%, the exponential is approximately unity and can be neglected, giving

$$Q_{v'}^{(\text{rot})}(T) = \frac{T}{c_2 B_{v'}}$$

2.2 Data Manipulation

The next project consisted of transferring SPIRE CVF data from Computer Center (CC) tapes to tapes with proper format for use on the APOLLO computer system. This involved reformatting the tapes and writing them without labels.

2.3 Program Modification

The final project consisted of modifying code to calculate the zenith auroral spectral intensity for NO and NO+ band systems. This involved adding subroutines to the zenith auroral programs already running, which calculated the spectrum at a given altitude. Once completed, the results of the zenith auroral spectral program are convolved with a Hamming window line shape and then plotted.

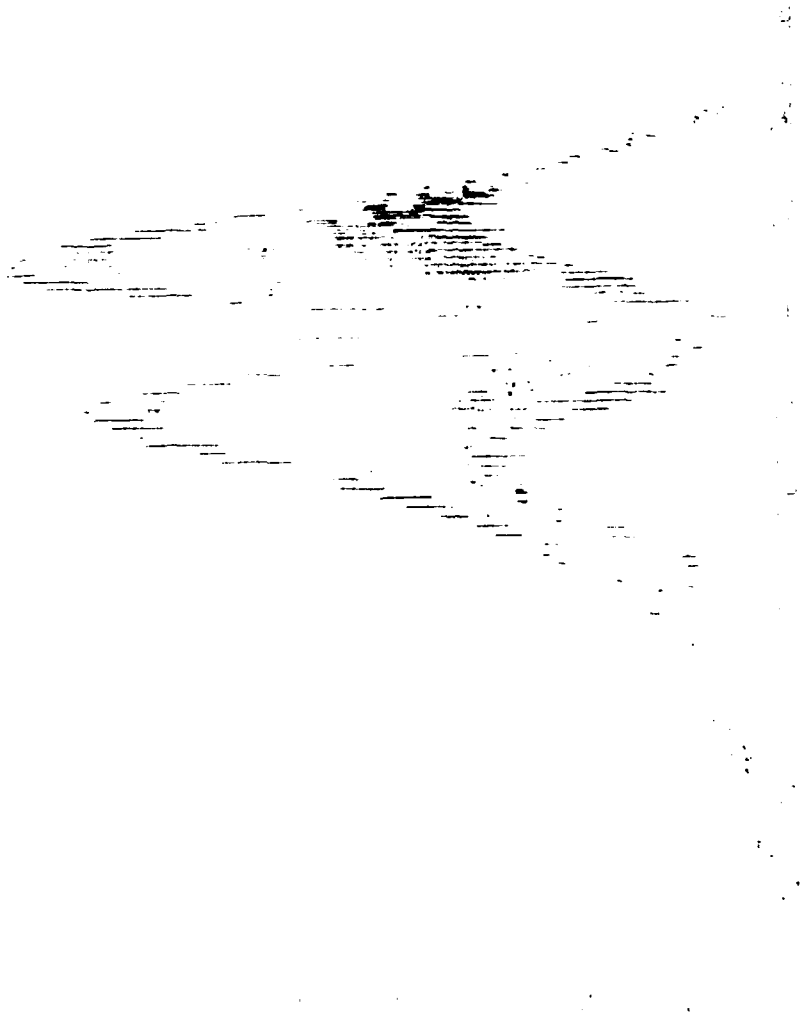


Figure 2.3.1.1 - Zenith Auroral Spectral Plot

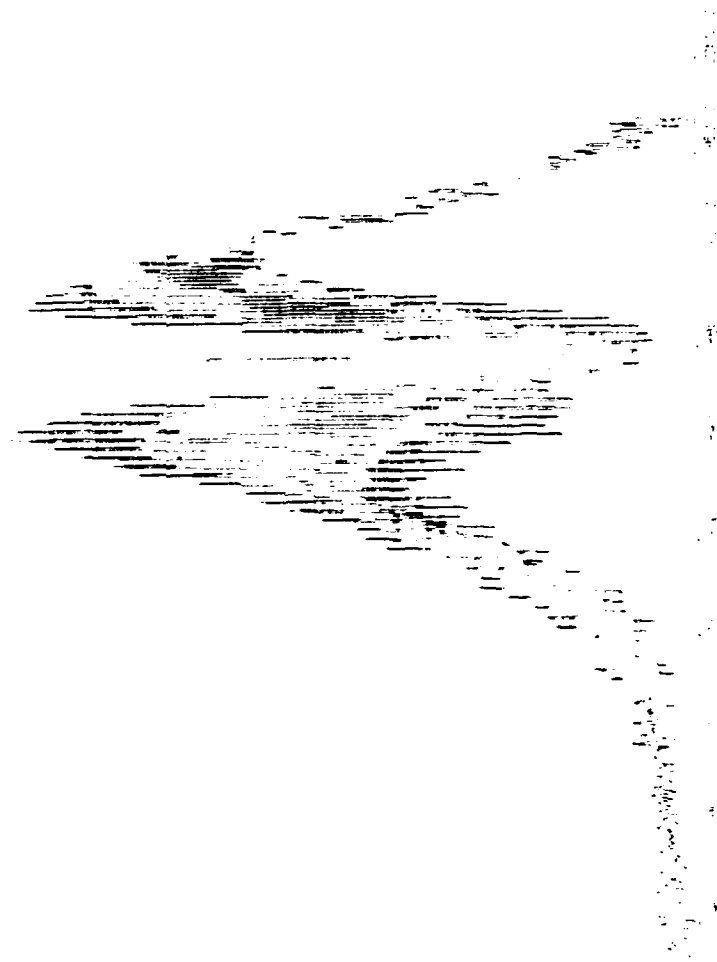


Figure 2.3.2 - Zenith Auroral Spectral Plot

BOREHOLE LOG PLOTTING AND ANALYSIS

1.0 OBJECTIVES

The objectives of this project were first to demonstrate that a program possessed by the Solid Earth Geophysics Branch (LWH) would reformat geophysical well data tapes. Secondly, a program to produce plots of the borehole log data using BEDFORD RESEARCH's graphic software was desired. Thirdly, any additional analyses were to be provided as required.

2.0 ANALYSIS

2.1 Data Conversion

The program SCFSCH converts geophysical well data written in Log Information Standard (LIS) format to Log Information Library (LIL) format. The program was written by Bendix Field Engineering Corporation, for the CDC system and was copied to the Cyber at the Air Force Geophysics Laboratory. To run SCFSCH, it was first necessary to type in a channel identification table provided in the documentation. A program was then written to copy the tape file to disk by buffering-in/buffering-out each record. Program SCFSCH can then be run as a batch job, attaching the necessary files, creating a file in LIL format and purging the original file in LIS format.

2.2 Plot Programs

The log plotting program (LOGPLOT) was written for the VAX. The program reads the well log files written in LIL format and plots the data requested by the user. The program utilizes BEDFORD RESEARCH graphics software. This enables the user to run LOGPLOT on either a VT125 or Tektronix terminal.

There are several options available with LOGPLOT. The user selects the log file and chooses the number and types of curves he wishes to plot. He also selects the depth ranges, the curve value ranges, and the scale factor for each axis. Additional options include the plotting of the center line and the selection of a linear or logarithmic curve axis. Figures 2.1, 2.2, and 2.3 show 3 log plots using the various options.

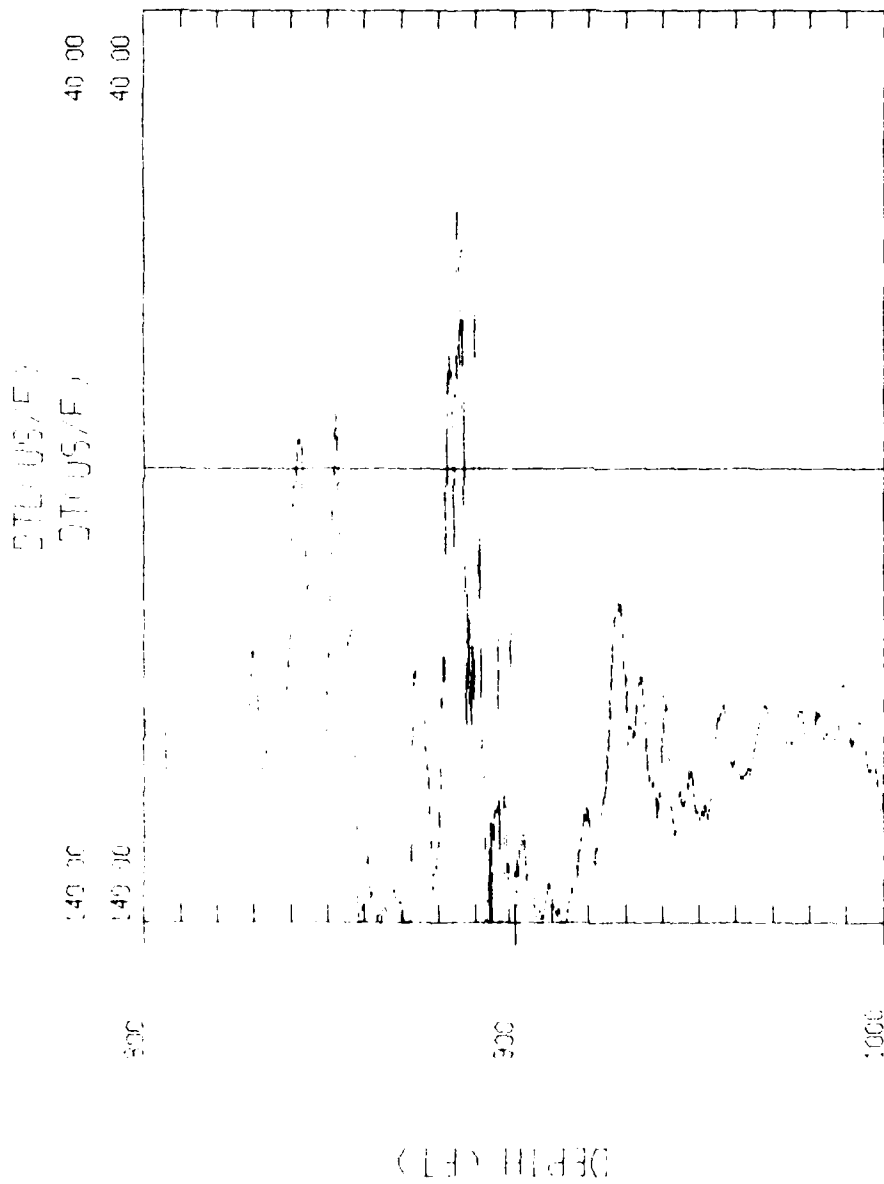


Figure 2.1 - Option 1: Linear Option Plot

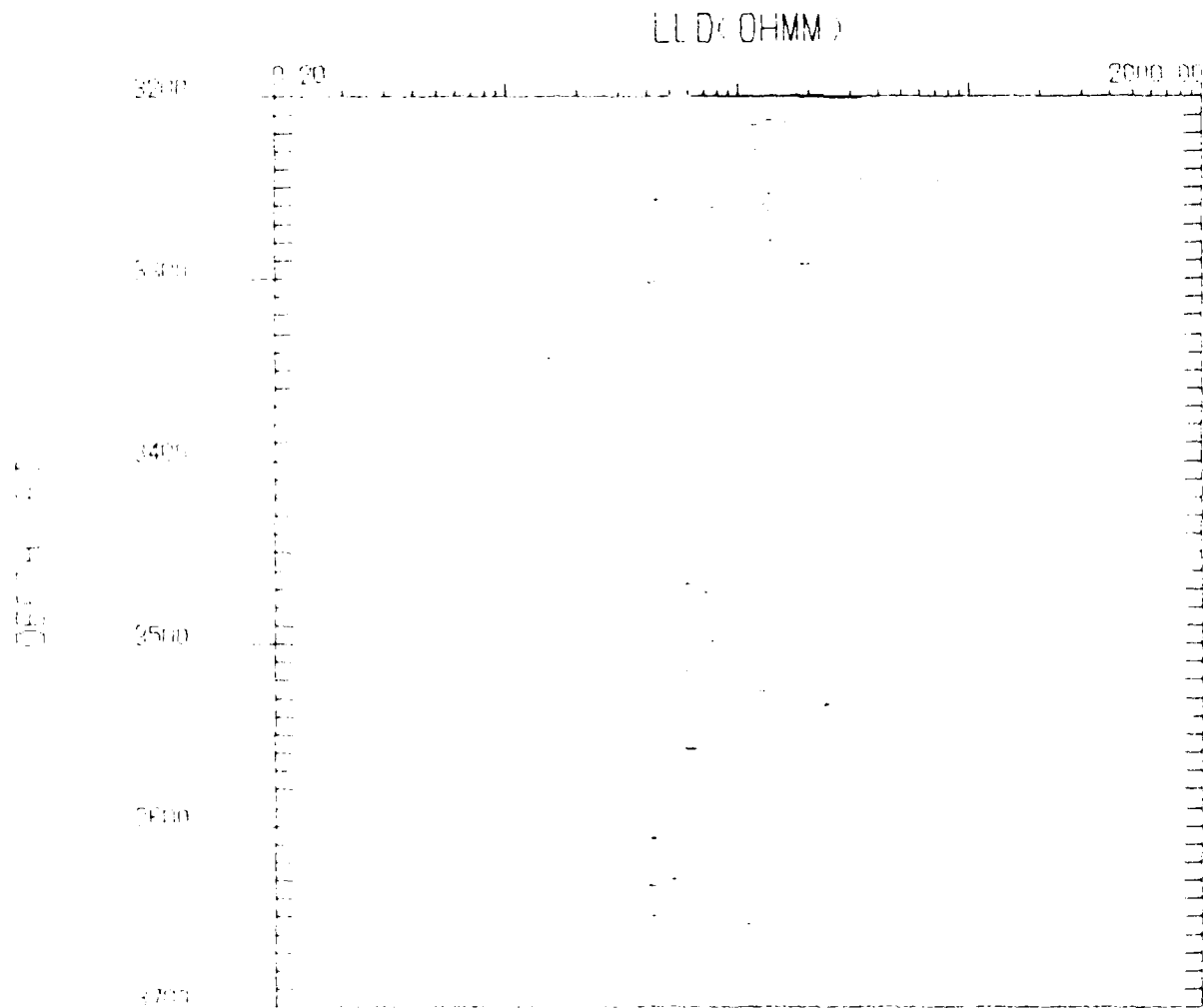


Figure 2.2 - Option 2; Log Option Plot

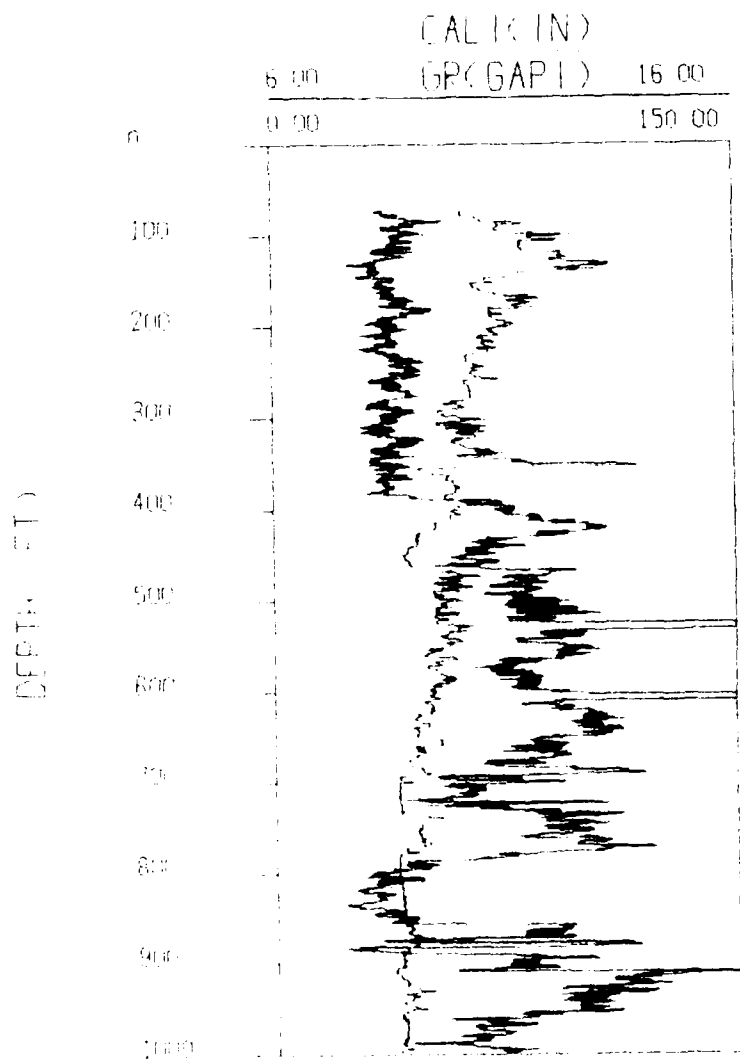


Figure 2.3 - Option 3: Third Option Plot

The plots on the VAX are produced after the log file in LIL format has been transferred from the CYBER. The plots can be printed on a hard copy unit, on 8 1/2 x 11 inch paper, with good resolution, resulting in a journal-quality figure. However, for research purposes, the optimal depth scale is 2.5 - 5 inches/100 feet. Since the boreholes range from approximately 2000 to 8000 feet deep, this necessitates plots that are at least 50 inches long. It would not be feasible to produce these plots on the VAX because there is no hard copying unit available for such lengthy plots. Therefore, the Initiator requested a version of LOGPLOT on the CYBER. This would enable the use of the Calcomp plotter, on which there is no limit to the length of the x (or depth) axis. The options are similar to those available on the VAX program, except that on the CYBER there is a maximum of 4 curves per plot since there are only 4 colored pens.

2.3 Interactive Programs

BEDFORD RESEARCH personnel wrote a procedure file for the CYBER which enables the Initiator to run programs SCFSCH and LOGPLOT easily. The procedure file runs interactively and allows the user to select one of three options: 1) copy an LIS tape to a disk file, 2) run SCFSCH, and 3) produce a log plot. The procedure prompts the user for the information necessary to generate a batch job for the particular option selected. After executing the procedure file, the batch job is submitted.

During the execution of program SCFSCH, only part of the information from the original LIS file is decoded. Therefore, the Initiator requested a program to edit the created LIL file and incorporate additional data such as the geographical coordinates of the borehole, the casing and logging information, etc. The resulting LILEDIT program on the VAX modifies 6 records and adds 5 records to the file in a format that meets LIL specifications.

3.0 SUMMARY

Research involving the well log data was also undertaken by REDFORD RESEARCH personnel. This involved two separate projects: 1) an analysis of tube waves in the cased Zeeck well and 2) a comparison of seismic velocities for 6 wells in the Texas Panhandle. Figure 3.1 shows the drift curves, the difference between the integrated sonic time and seismic time for the wells. The preliminary analysis for these projects was completed but the projects were not brought to their final completion, due to complications and lack of time.

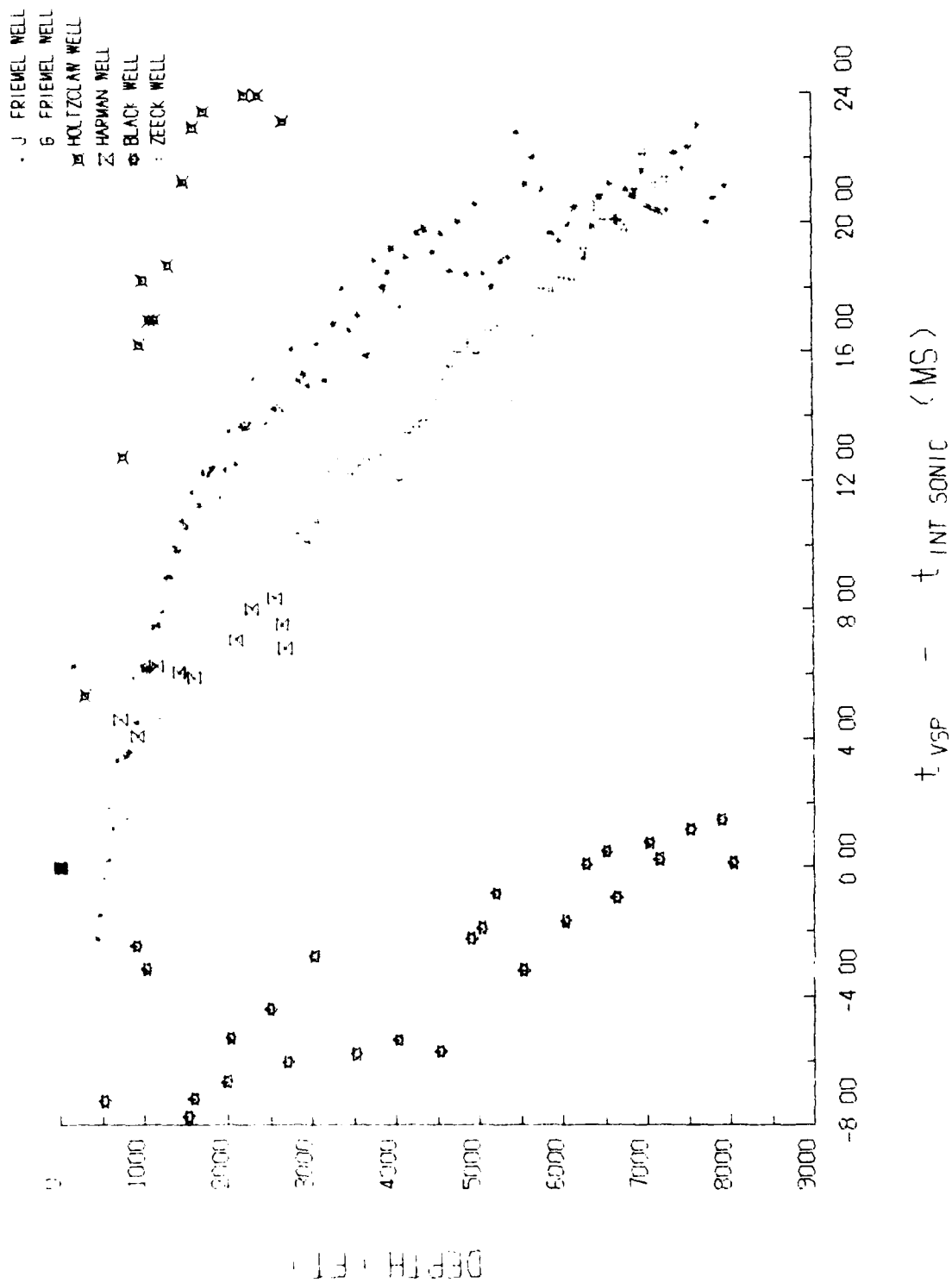


Figure 3.1 - Drift Curve

END

DATE

7-86